Cell Reports

Article

The *Drosophila* Ortholog of Mammalian Transcription Factor Sox9 Regulates Intestinal Homeostasis and Regeneration at an Appropriate Level

Graphical Abstract

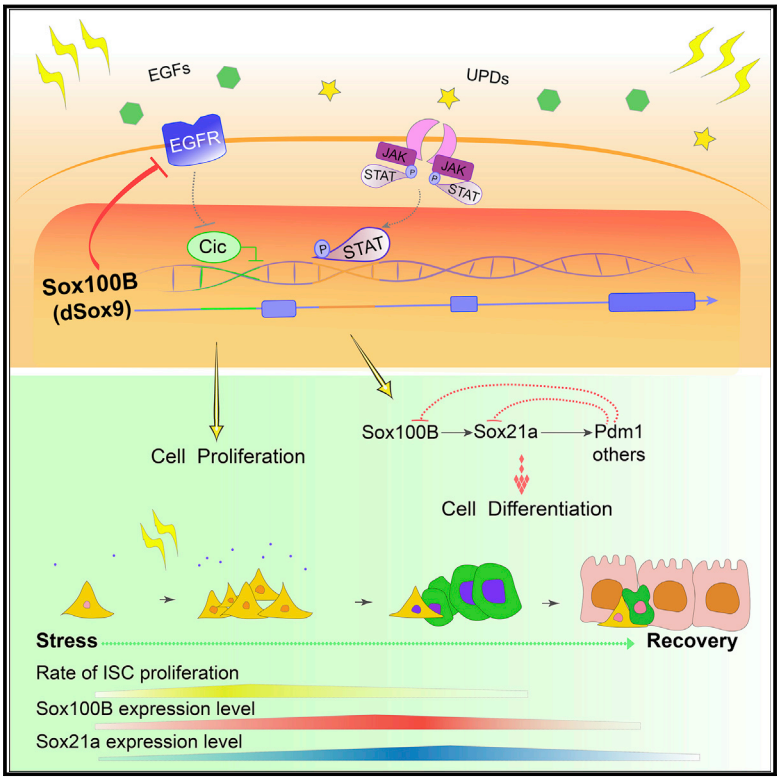

Highlights

- dSox9/Sox100B promotes ISC proliferation only at an appropriate level
- Sox100B is directly induced by both JAK/STAT and EGFR/Ras signaling pathways
- Sox100B overexpression inhibits MAPK signaling by suppressing EGFR expression
- Sox100B promotes cell differentiation via a Sox100B-Sox21a-Pdm1 regulatory circuitry

Authors

Zhen Jin, Jun Chen, Huanwei Huang, ..., Yongchao Zhang, Tao Cai, Rongwen Xi

Correspondence

xirongwen@nibs.ac.cn

In Brief

Jin et al. report that the *Drosophila* Sox9 ortholog functions downstream of EGFR and JAK/STAT signaling pathways, and that its expression modulation is critical for coordinated ISC proliferation and differentiation during intestinal homeostasis and regeneration.

Jin et al., 2020, Cell Reports *31*, 107683
May 26, 2020
https://doi.org/10.1016/j.celrep.2020.107683

CellPress

Cell Reports

CellPress
OPEN ACCESS

Article

The *Drosophila* Ortholog of Mammalian Transcription Factor Sox9 Regulates Intestinal Homeostasis and Regeneration at an Appropriate Level

Zhen Jin,[1,2] Jun Chen,[2] Huanwei Huang,[2] Jiawen Wang,[2] Jiaying Lv,[2] Menghan Yu,[2] Xingting Guo,[2] Yongchao Zhang,[2] Tao Cai,[2] and Rongwen Xi[2,3,4,*]

[1]College of Life Sciences, Beijing Normal University, Beijing 100875, China
[2]National Institute of Biological Sciences, No. 7 Science Park Road, Zhongguancun Life Science Park, Beijing 102206, China
[3]Tsinghua Institute of Multidisciplinary Biomedical Research, Tsinghua University, Beijing 102206, China
[4]Lead Contact
*Correspondence: xirongwen@nibs.ac.cn
https://doi.org/10.1016/j.celrep.2020.107683

SUMMARY

Balanced stem cell self-renewal and differentiation is essential for maintaining tissue homeostasis, but the underlying mechanisms are poorly understood. Here, we identified the transcription factor SRY-related HMG-box (Sox) 100B, which is orthologous to mammalian Sox8/9/10, as a common target and central mediator of the EGFR/Ras and JAK/STAT signaling pathways that coordinates intestinal stem cell (ISC) proliferation and differentiation during both normal epithelial homeostasis and stress-induced intestinal repair in *Drosophila*. The two stress-responsive pathways directly regulate Sox100B transcription via two separate enhancers. Interestingly, an appropriate level of Sox100B is critical for its function, as its depletion inhibits ISC proliferation via cell cycle arrest, while its overexpression also inhibits ISC proliferation by directly suppressing EGFR expression and additionally promotes ISC differentiation by activating a differentiation-promoting regulatory circuitry composed of Sox100B, Sox21a, and Pdm1. Thus, our study reveals a Sox family transcription factor that functions as a stress-responsive signaling nexus that ultimately controls tissue homeostasis and regeneration.

INTRODUCTION

Homeostatic renewal of many adult tissues requires balanced stem cell proliferation and differentiation, a process that is commonly compromised in cancer and in tissue degenerative diseases. The intestinal epithelium in adult *Drosophila* midgut provides a genetically tractable system for understanding the underlying mechanisms of tissue homeostasis and regeneration driven by resident stem cells (Biteau et al., 2011; Jiang and Edgar, 2011). The intestinal stem cells (ISCs) of the *Drosophila* midgut normally divide to renew themselves and give rise to two different types of progenitor cells that respectively differentiate into enterocyte cells (ECs) and enteroendocrine cells (EEs) (Figure 1A; Chen et al., 2018; Micchelli and Perrimon, 2006; Ohlstein and Spradling, 2006, 2007). Normally, ISCs divide occasionally and thereby maintain the ongoing renewal of the epithelium, a slow process that takes approximately 2–4 weeks. However, upon damage or infection, ISCs are able to rapidly divide to facilitate accelerated epithelial repair in as fast as two days (Amcheslavsky et al., 2009; Buchon et al., 2009b; Chen et al., 2016; Jiang et al., 2009).

Extensive studies have implicated the JAK/STAT and the EGFR/Ras/mitogen-activated protein kinase (MAPK) as the two major signaling pathways that regulate ISC proliferation and differentiation during both normal epithelial homeostasis and stress-induced intestinal repair (Beebe et al., 2010; Biteau and Jasper, 2011; Buchon et al., 2009a, 2010; Jiang et al., 2009, 2011; Jin et al., 2015; Liang et al., 2017; Lin et al., 2010; Xu et al., 2011). The EGFR signaling is considered to play a predominant role in the regulation of ISC proliferation because it is required for the JAK/STAT signaling activation-induced ISC proliferation, whereas the JAK/STAT signaling is not essential for EGFR/Ras signaling activation-induced ISC proliferation (Cordero et al., 2012a; Jiang et al., 2011). The EGFR signaling is also important for remodeling of the differentiated cells, including the exclusion of damaged/aged ECs and incorporation of new cells (Buchon et al., 2010). The JAK/STAT pathway is also essential for ISC differentiation. ISCs with compromised JAK/STAT activity generate progenitor cells that are incapable of further differentiation (Beebe et al., 2010; Jiang et al., 2009; Lin et al., 2010). Despite the importance of the two signaling pathways in controlling intestinal homeostasis, their downstream targets—which integrate pathway activities to coordinate ISC proliferation and differentiation—remain elusive.

Sox (SRY-related HMG-box) family transcription factors (TFs) are known to have diverse roles in cell-fate specification and differentiation in multicellular organisms (Kamachi and Kondoh, 2013; Sarkar and Hochedlinger, 2013). In mouse-small intestine, Sox9,

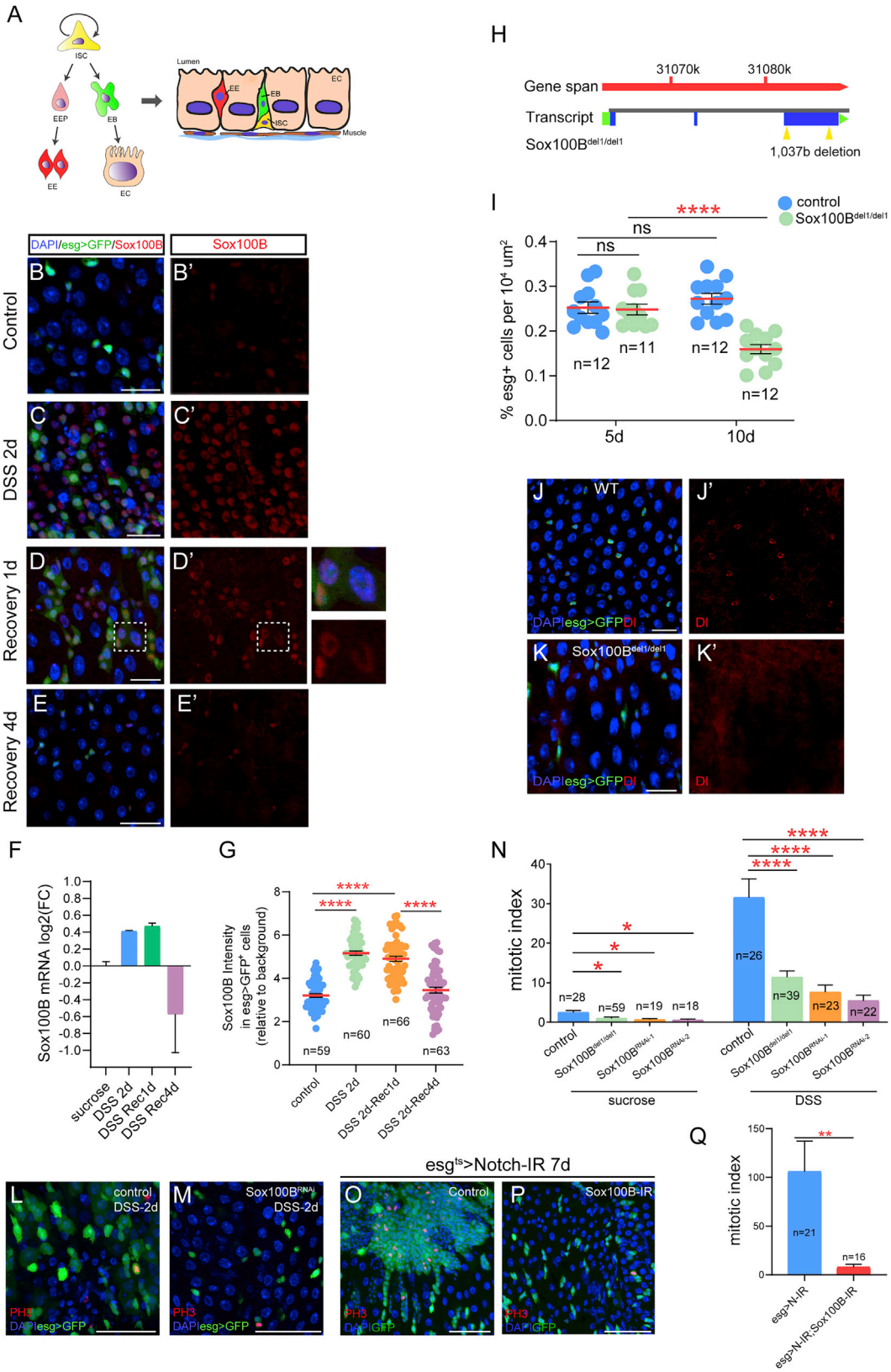

(legend on next page)

a SoxE subfamily member, is expressed in ISCs to regulate ISC proliferation and differentiation, but whether it acts as an oncogene or a tumor suppressor is still in debate (Bastide et al., 2007; Mori-Akiyama et al., 2007; Prévostel and Blache, 2017). In *Drosophila* midgut, Sox21a, a SoxB2 subfamily member, is specifically expressed in ISCs and transient progenitor cells, and is essential for progenitor cell differentiation into mature cells (Chen et al., 2016; Zhai et al., 2015, 2017). Here we identified Sox100B, the *Drosophila* ortholog of *Sox9*, as a common downstream gene target for both the JAK/STAT and the EGFR signaling in regulating ISC proliferation and differentiation. We also revealed that an appropriate level of Sox100B is critical for its function in regulating ISC proliferation, in that it may allow it to serve as an important mediator for a balanced process of ISC proliferation and differentiation, thereby maintaining intestinal homeostasis.

RESULTS

Sox100B Is a Stress-Responsive Transcription Factor Expressed in Intestinal Progenitor Cells

Previous gene expression analyses have indicated stem/progenitor cell-specific expression of Sox100B in the *Drosophila* midgut (Amcheslavsky et al., 2014; Doupé et al., 2018; Dutta et al., 2015). We generated a polyclonal antibody against Sox100B, and immunostaining with this antibody revealed weak but discernible Sox100B expression in Dl^{+} ISCs, and enteroblasts (EBs), the committed progenitor cells that are marked by the Notch activation reporter NRE-Gal4, UAS-GFP (NRE>GFP for short; Figure S1A). A similar expression pattern was found with a GFP-tagged Sox100B bacterial artificial chromosome/clone (BAC) transgene (Kudron et al., 2018; Figure S1B).

We found a strongly increased Sox100B expression pattern in some randomly occurred regions that displayed abnormal cell clusters (Figure S1C), indicating that Sox100B expression may be stress-responsive. Interestingly, expression of Sox100B was upregulated in progenitor cells after a continuous 48-h dextran sulfate sodium (DSS) treatment (Amcheslavsky et al., 2009), when intensive ISC proliferation was occurring (Figures 1B–1G and S1D–S1G). After 24 h of recovery time, when massive cell differentiation was occurring, Sox100B showed sustained high expression level in the differentiating ECs (Figures 1D–1G and S1D–S1G). Its expression returned to normal level at day 4 after DSS treatment (Figures 1E–1G). We also examined Sox100B expression during regeneration induced by feeding flies with *Pseudomonas entomophilia* (P.e.), a bacterial species that is highly pathogenic to *Drosophila* (Jiang et al., 2009; Vodovar et al., 2005). We observed a similar dynamic expression pattern of Sox100B during the process: its expression was dramatically upregulated during the infection and early recovery phases and returned to normal at day 4 after the infection was stopped (Figures S1H–S1L). These results indicate a potential role for Sox100B in intestinal regeneration in response to diverse types of stresses.

Sox100B Is Required for ISC Proliferation and Intestinal Regeneration

Using the CRISPR-Cas9 system, we generated a Sox100B mutation strain *Sox100B*^{del1}, with a large deletion on the *Sox100B* coding region. Immunostaining with anti-Sox100B antibody showed absence of any signal in the midgut of the homozygous mutant flies (Figures S1M and S1N), indicating that *Sox100B*^{del1} is a genetic null allele of *Sox100B*.

Using an ISC- and EB-specific driver (Escargot [Esg]-Gal4, UAS-GFP, abbreviated as "esg>GFP") as a reporter for progenitor cells (Micchelli and Perrimon, 2006), we found that *Sox100B*^{del1}/*Sox100B*^{del1} homozygous gut showed an age-dependent decline of progenitor cells (Figure 1I). In addition, Dl became barely visible (Figures 1J and 1K), indicating that Sox100B is required for long-term maintenance of ISCs. Staining with cleaved Dcp-1, an apoptosis marker, revealed that there was no significant increase in the incidence of apoptosis in the mutant progenitor cells (Figures S3A–S3C), suggesting that the loss of ISC is not caused by cell death. Phospho-Histone 3 (PH3) quantification revealed reduced homeostatic proliferation in both *Sox100B*^{del1}/*Sox100B*^{del1} guts and in Sox100B-RNAi guts (esg^{ts}>Sox100B-RNAi and Dl^{ts}>Sox100B-RNAi), as well as impaired regenerative proliferation in response to DSS treatment or P.e. infection (Figures 1L–1N, S1O–S1R, and S2A–S2D). As reduced cell proliferation

Figure 1. Sox100B Is Required for ISC Proliferation in Both Normal and Stress Conditions

(A) Schematic diagram of the ISC lineage and intestinal epithelium in *Drosophila*.

(B–E) Midguts stained with anti-Sox100B antibody (red) in flies fed with sucrose (B and B′) or DSS (C and C′) for two days, then after recovery for one day (D and D′), and after recovery for four days (E and E′). Separated color channels for the insets (D and D′) were enlarged and displayed on the right, showing the Sox100B expression in pre-mature EBs.

(F) Quantitative real-time PCR results of Sox100B mRNA levels in midguts of flies following sucrose, DSS for two days, recovery for one day, and recovery for four days. Three independent replicates were carried out for each sample.

(G) Quantitative analysis of fluorescence intensity for anti-Sox100B staining in progenitor cells in the midgut treated with sucrose, DSS for two days, recovery for one day, and recovery for four days.

(H) A diagram describing the molecular lesion of the *Sox100B* mutant allele, *Sox100B*^{del1}.

(I) Quantification for the percentage of Esg^{+} progenitor cells in the midgut (every 3 x 10^4 μm^2) of flies five days or 10 days after eclosion.

(J and K) Midguts of *esg*^{ts}*>GFP* (J and J′) and *esg*^{ts}*>GFP; Sox100B*$^{del1/del1}$ (K and K′) flies stained with DAPI (blue) and anti-Dl (red) antibody 10 days after eclosion.

(L and M) Midguts stained with DAPI (blue) and anti-Phospho histone 3 (PH3, red) in *esg*^{ts}*>GFP* (L) or *esg*^{ts}*>Sox100B-RNAi* (M) flies that were treated with DSS for two days.

(N) Mitotic index analysis via quantification of PH3^{+} cells in midgut of flies. Wild-type (WT), *Sox100B*$^{del1/del1}$, *esg*^{ts}*>Sox100B-RNAi-1*, and *esg*^{ts}*>Sox100B-RNAi-2* flies treated for two days of sucrose or DSS were collected for analysis.

(O–Q) Midguts of the following genotypes of flies stained with DAPI (blue) and anti-PH3(red): *esg*^{ts}*>N-IR* (O) and *esg*^{ts}*>N-IR;Sox100B-IR* (P) flies. Mitotic index analysis via quantification of PH3^{+} cells (Q). Flies were shifted to restrictive temperature for seven days before analysis.

n is as indicated. Significance was measured with unpaired two-tailed t tests. Mean ± SEM. $^{ns}p > 0.05$; $^{*}p < 0.05$; $^{**}p < 0.01$; $^{****}p < 0.0001$. Scale bars, 50 μm in (L), (M), (O), and (P), and 20 μm in others. See also Figures S1, S2, and S3.

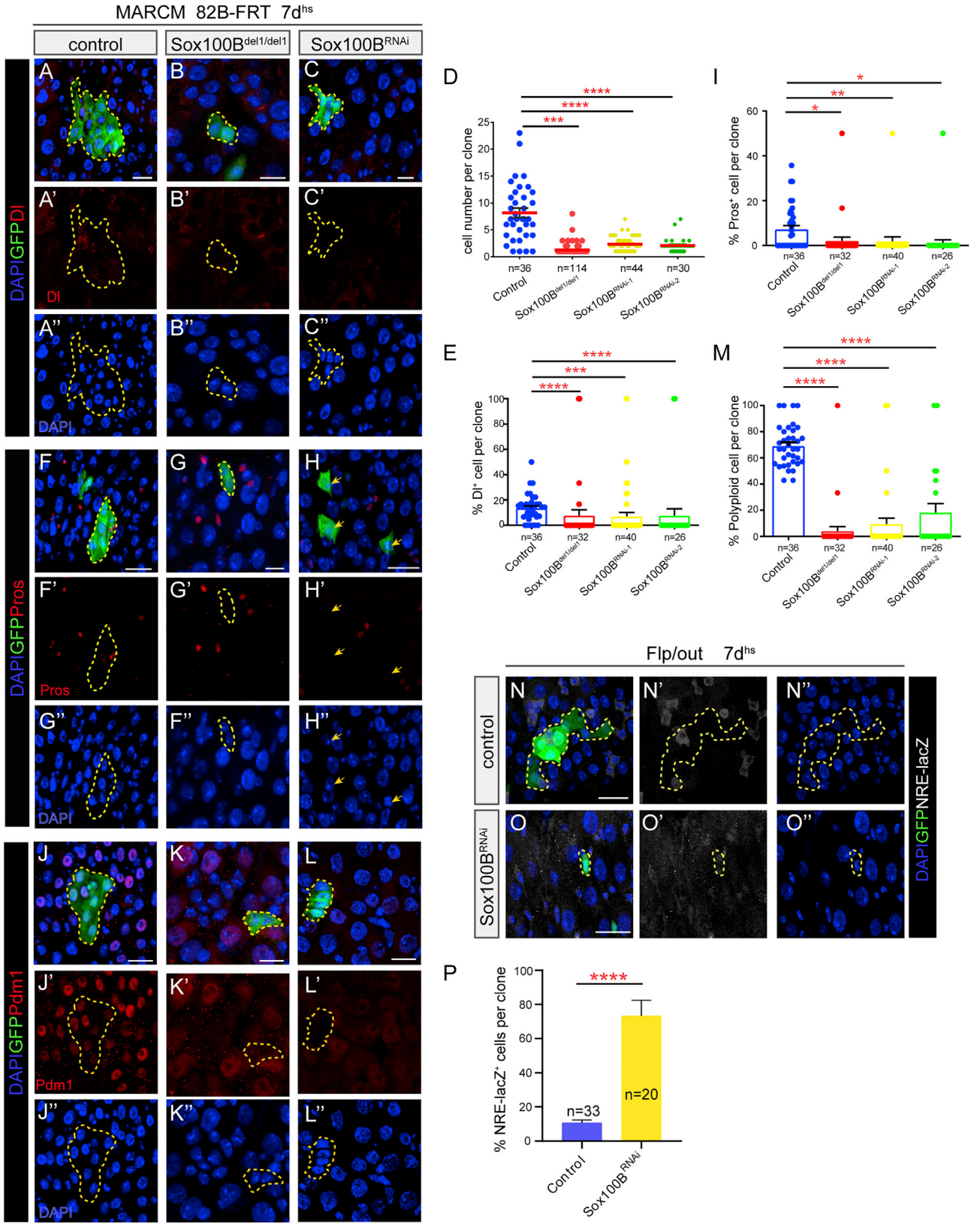

(legend on next page)

phenotype in gut could be secondary to ISC loss, we examined the effect of Sox100B depletion on the development of *Notch* mutant ISC-like tumors (Micchelli and Perrimon, 2006; Ohlstein and Spradling, 2006). Depletion of Sox100B in esg>GFP$^+$ cells dramatically suppressed the tumor development, and the density and distribution of esg>GFP$^+$ cells became largely comparable to the wild-type midgut (Figures 1O–1Q). These observations demonstrate that Sox100B is required for ISC proliferation and long-term maintenance under both normal and stress conditions.

As Sox100B-depleted ISCs seem to enter a quiescent state, we also used the FLY-FUCCI system (Zielke et al., 2014) to examine the cell cycle status of Sox100B-depleted ISCs. Interestingly, compared to normal ISCs, the mutant ISCs showed significant increase in S-phased cells. This observation indicates that the reduced cell proliferation of Sox100B-depleted ISCs may be due to a delay in S phase or S to G2 transition (Figures S2E and S2F).

Sox100B Is Required for Progenitor Cell Differentiation

We observed that all *Sox100B*^{del} homozygous clones generated by the MARCM system showed significantly smaller clone size compared to wild-type clones (Figures 2A, 2B, and 2D). Knocking down Sox100B by RNAi in clones produced largely similar phenotypes, except that the RNAi clones could grow slightly larger than *Sox100B* null clones, possibly due to incomplete depletion of Sox100B (Figures 2C and 2D). Overexpression of a potent apoptosis inhibitor p35 failed to rescue the reduced-clone-size phenotype, further suggesting that the defect is not caused by cell death (Figures S3E–S3I).

Staining with various cell markers, including Dl (Figures 2A–2E), Pros (the EE marker) (Figures 2F–2I), and Pdm1 (the EC marker) (Figures 2J–2M) revealed that the mutant or RNAi cells were negative for all of these cell markers. As most of these mutant cells remained as diploid cells, they are probably arrested at an EB-like cell stage. Indeed, by using Flp/out system, we found an increase in NRE-lacZ$^+$ cells in Sox100B-depleted clones (Figures 2N–2P). Normally, ISCs and EBs exhibit in pairs with one ISC and one EB juxtaposed with each other, and this pattern is quickly changed to ISC-like (Dl$^+$/Dl$^+$) pairs following damage, likely due to increased ISC proliferation/self-renewal (Zhai et al., 2017). We found that this Dl$^+$/Dl$^+$ pair phenotype was blocked when Sox100B was depleted. Instead, most progenitor cells exhibited Dl$^+$/NRE-lacZ$^+$ pairs or single Dl$^+$ or NRE-lacZ$^+$ cells, indicating a suppressed ISC proliferation and a precocious differentiation of ISC to EB fate (Figures S3J–S3M). These results collectively suggest that loss of Sox100B causes ISCs to be arrested in cell cycle progression and lose Dl expression, and these mutant cells are unable to terminally differentiate but rather they are arrested at an undifferentiated progenitor cell stage.

Sox100B Is Regulated in Parallel by JAK/STAT and EGFR Signaling Pathways

We next sought to understand how Sox100B is regulated. After screening through a number of signaling transduction pathways that are known to be involved in ISC proliferation and/or differentiation, including the JAK/STAT, EGFR/Ras/MAPK, as well as JNK, Hippo, and Wnt/Wg signaling pathways (Biteau et al., 2008; Biteau and Jasper, 2011; Buchon et al., 2009a, 2010; Jiang et al., 2009, 2011; Karpowicz et al., 2010; Liang et al., 2017; Lin et al., 2008, 2010; Ren et al., 2010; Shaw et al., 2010; Xu et al., 2011), we identified the JAK/STAT and the EGFR/Ras/MAPK signaling pathways as the ones whose transient alteration in their activity caused robust change of Sox100B expression in progenitor cells.

We activated the JAK/STAT pathway by overexpression of Hop (a *Drosophila* homolog of JAK) or by induction of ligand Upd. The EGFR signaling pathway was activated by overexpression of EGFR$^{top4.2}$ (active form of EGFR) or Ras^{V12} (active form of Ras). To minimize secondary effects caused by sustained activation of JAK/STAT or EGFR pathways, we treated flies for only 48 h before examination. Overactivation of either the JAK or EGFR pathways in ISCs and EBs significantly upregulated Sox100B expression (Figures 3A–3I and S4A–S4D). Overexpression of Dome^{DN} (a dominant-negative form of *Dome*, the JAK/STAT receptor) and/or RNAi silencing of EGFR to inactivation of either of these two signaling pathways effectively downregulates Sox100B expression (Figures 3A–3I). We additionally found that activation of either of these two pathways with simultaneous inhibition of the other was still able to upregulate Sox100B (Figures 3F–3I). Moreover, ectopic activation of the JAK or EGFR pathway in EC cells driven by the Myo1A-Gal4 driver was sufficient to induce expression of Sox100B in EC cells (Figures 3J

Figure 2. Sox100B Is Required for ISC Differentiation

Midgut carrying MARCM clones (GFP, green) examined seven days after clone induction. Dashed lines depict clone margins, and arrows indicate cells inside of the clones.

(A–C) MARCM clones co-stained with DAPI (blue) and anti-Dl (red). (A–A″) WT *FRT82B* clone, (B–B″) *Sox100B*$^{del1/del1}$ *FRT82B* clone, and (C–C″) *Sox100B-RNAi FRT82B* clone.

(D) Quantification of the cell number per clone.

(E) Quantification of the proportion of Dl$^+$ cells per clone.

(F–H) MARCM clones co-stained with DAPI (blue) and anti-Pros (red). (F–F″) WT *FRT82B* clone, (G–G″) *Sox100B*$^{del1/del1}$ *FRT82B* clone, and (H–H″) *Sox100B-RNAi FRT82B* clones.

(I) Quantification of the proportion of Pros$^+$ cells per clone.

(J–L) MARCM clones co-stained with DAPI (blue) and anti-Pdm1 (red). (J–J″) WT *FRT82B* clone, (K–K″) *Sox100B* $^{del1/del1}$ *FRT82B* clones, and (L–L″) *Sox100B-RNAi FRT82B* clones.

(M) Quantification of the proportion of polyploid cells per clone.

(N and O) Flp/out clones co-stained with DAPI (blue) and anti-lacZ (white). (N–N″) WT clone and (O–O″) *Sox100B-RNAi; NRE-lacZ* clone.

(P) Quantification of the proportion of NRE-lacZ$^+$ cells per clone.

n is as indicated. Significance was measured with unpaired two-tailed t tests. Mean ± SEM. *p < 0.05; **p < 0.01; ***p < 0.001; ****p < 0.0001. Scale bars, 20 μm for (N) and (O), and 10 μm for others. See also Figures S2 and S3.

and 3K), indicating an autonomous regulatory mechanism. Furthermore, the upregulated expression of Sox100B induced by DSS stress was significantly suppressed following either EGFR or JAK pathway inhibition (Figures S4E–S4G). Collectively, these results indicate that these two signaling pathways function in parallel to positively regulate Sox100B expression.

A further point to consider is how these two signaling pathways regulate Sox100B. Interestingly, the Capicua (Cic) DamID profile from a previous study indicates several Cic-binding sites in the promoter region (termed here as the "E1" region) of Sox100B (Figure 3L; Jin et al., 2015). Cic is known to act downstream of EGFR/Ras/MAPK to regulate ISC proliferation, and is phosphorylated by MAPK. Phosphorylation of Cic causes its nucleus-to-cytoplasm translocation and consequently the depression of Cic target genes (Jin et al., 2015). We generated a lacZ-reporter line driven by this E1 region, named as *Sox100B-lacZ*^{E1}, which showed a weak but progenitor-specific expression pattern that is similar to Sox100B (Figures 3L and 3M). We found that *cic* negatively regulated Sox100B expression in intestinal progenitor cells (Figures S4H–S4L). In addition, the *Sox100B-lacZ*^{E1} reporter was responsive to EGFR signaling activity: activation of EGFR in ISCs promoted its expression, whereas inhibition of EGFR suppressed its expression (Figures 3M and 3N).

Further analysis on the regulatory regions of Sox100B revealed three putative STAT-binding sites (TTCN$_{3/4}$GAA, named as 4n1, 3n, and 4n2, respectively) within the first intron (termed here as the "E2" region) of Sox100B (Figure 3L). The resultant *Sox100B-lacZ*^{E2} reporter driven by the E2 region also showed a similar progenitor-cell-specific expression pattern (Figure 3O). Importantly, overexpression of Hop in progenitor cells dramatically upregulated *Sox100B-lacZ*^{E2} expression, while overexpression of Dome^{DN} downregulated *Sox100B-lacZ*^{E2} expression (Figures 3O and 3P). In contrast, neither the increased nor the decreased EGFR pathway activity caused any obvious effect on Sox100B-lacZ^{E2} expression level (Figures 3O and 3P), showing that the E2 enhancer region is specifically responsive to JAK/STAT. Further mutational analysis revealed that a double mutation of 4n1 and 4n2 sites, but not either one alone, completely eliminated progenitor cell expression of lacZ, and this occurred both in normal midgut- and under DSS-induced stress conditions (Figures 3Q, 3R, and S4M–S4Q), suggesting that JAK/STAT signaling directly targets Sox100B via these two 4n sites in the E2 enhancer region. Collectively, these data suggest that both EGFR/Ras/Cic and JAK/STAT signaling pathways directly regulate Sox100B expression via the E1 and E2 enhancer regions, respectively (Figure 3S).

Sox100B Is Required for JAK/STAT and EGFR Signaling Activation-Induced ISC Proliferation

We next performed epistatic analyses to determine whether Sox100B mediates the JAK/STAT and EGFR signaling pathways to regulate ISC proliferation. Knockdown of Sox100B effectively suppressed the accumulation of esg^{+} cells induced by overexpression of Upd or EGFR$^{top4.2}$ (Figures 4A–4F). Mitotic index analysis confirmed that knockdown of Sox100B significantly suppressed the JAK/STAT- and EGFR-activated ISC proliferation (Figure 4G).

Consistent with the requirement for JAK/STAT pathway in progenitor cell differentiation, inactivation of the JAK/STAT signaling pathway by overexpression of Dome^{DN} generated cell clusters containing differentiation-defective progenitor cells in the midgut epithelium (Figures 4H and 4K). Interestingly, co-overexpression of Sox100B with Dome^{DN} not only effectively suppressed this undifferentiated cell cluster phenotype, but also allowed many cells to differentiate into Pdm1^{+} ECs (Figures 4I–4M). Taken together, these observations suggest that Sox100B functions downstream of the JAK/STAT and EGFR signaling pathways to regulate both ISC proliferation and differentiation. Given its functional importance, Sox100B is likely a key downstream mediator of these two pathways in controlling ISC proliferation and differentiation.

Overexpression of Sox100B Inhibits ISC Proliferation via a Feedback Mechanism

Considering that loss of Sox100B causes ISC quiescence, we next asked whether overexpression of Sox100B is sufficient to induce ISC proliferation. Unexpectedly, overexpression of a UAS-Sox100B transgene using the esg^{ts}-Gal4 or Dl^{ts}-Gal4 driver did not give rise to any obvious phenotype, except that the mitotic index of the intestine was slightly lower to the wild-type control (Figures 5A, S2C, and S2D). Surprisingly, overexpression of Sox100B almost completely blocked the proliferation response following DSS treatment or *P.e.* infection (Figures 5A–5C and S1O–S1R). Sox100B overexpression also strongly suppressed *Notch*-depletion-induced intestinal-tumor formation (Figures S2G–S2I). Moreover, the Sox100B-overexpressed MARCM clones showed significantly smaller sizes, with only approximately two cells on average per clone compared to eight cells per wild-type clone (Figures 5D–5G), and this reduced clone size is not caused by increased cell death (Figures S3D and S3G). Therefore, overexpression of Sox100B, and likewise depletion of Sox100B, both resulted in suppression of ISC proliferation. Interestingly, as revealed by Fly-FUCCI, overexpression of Sox100B caused significant increase in cells in the G1 phase (Figures S2E and S2F), indicating a cell cycle arrest in the G1 phase, which is in contrast to an arrest in the S phase caused by Sox100B depletion. Therefore, the mechanisms for the reduced ISC proliferation caused by Sox100B overexpression and Sox100B depletion might be different.

As overexpression of Sox100B, and likewise depletion of Sox100B, both resulted in suppression of ISC proliferation, a "just-right" expression level of Sox100B is required for proper intestinal homeostasis and regeneration. To test this "just-right" hypothesis, we managed to induce different levels of Sox100B expression in ISCs by culturing flies with the Gal4^{ts}-UAS expression system at different temperatures (18°C, 22°C, 25°C, and 29°C). Interestingly, the highest mitotic indexes were found in growing flies at 22°C, and the second highest at 25°C, while flies cultured at 18°C or 29°C both showed minimal mitotic activity (Figure 5H). In addition, in contrast to the dampened ISC proliferation effect caused by either UAS-Sox100B or UAS-Sox100B-RNAi expression, the mixed expression of UAS-Sox100B and UAS-Sox100B-RNAi, which presumably produces intermediate levels of Sox100B expression, induced significant ISC overproliferation (Figure S2J). Collectively, these data strongly support a "dosage effect" of Sox100B: an appropriate level of Sox100B is critical for ISC proliferation.

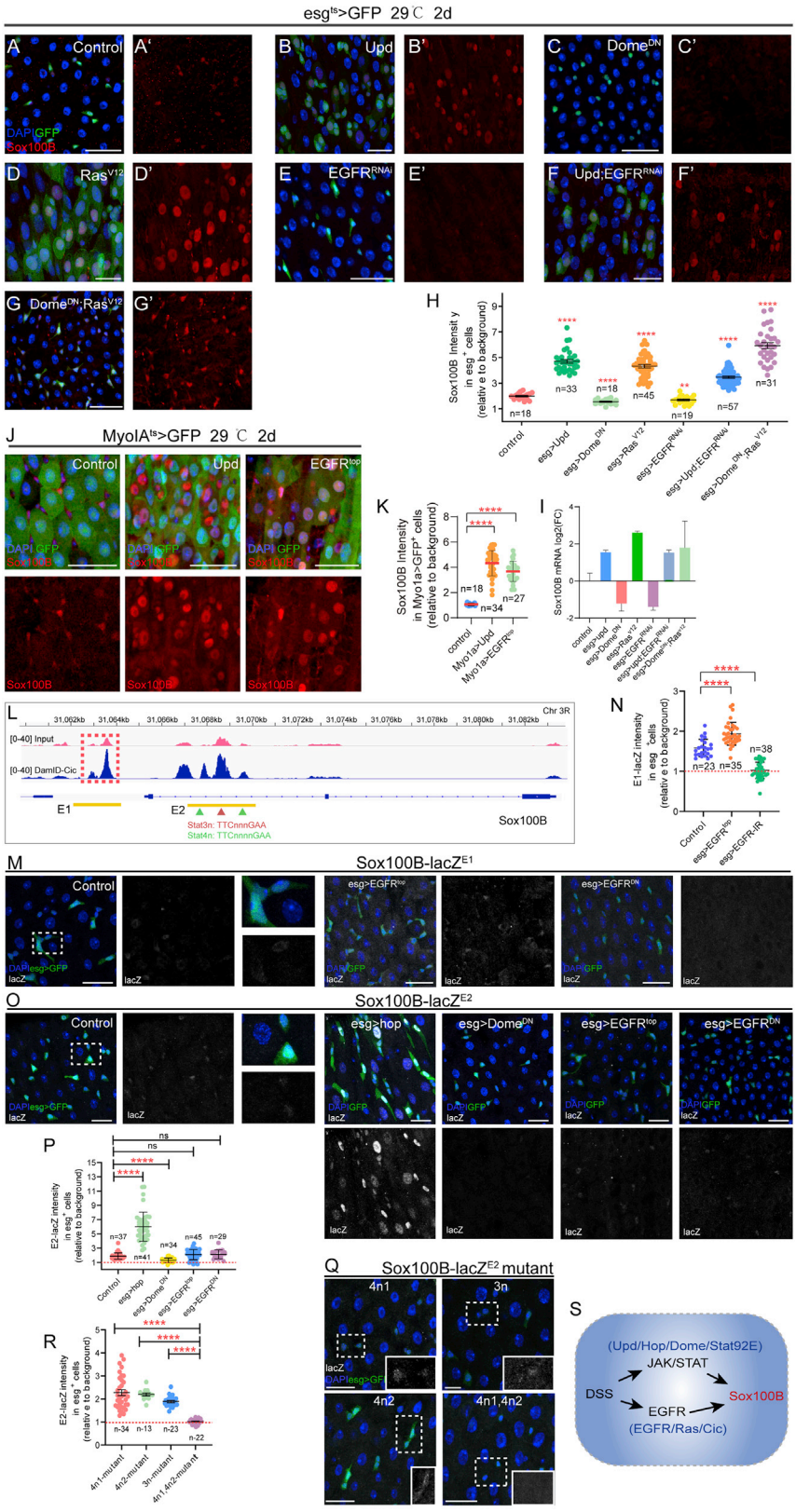

Figure 3. Sox100B Is Regulated in Parallel by JAK/STAT and EGFR Signaling Pathways

(A–G) Midguts expression of GFP (green) co-stained with DAPI (blue) and anti-Sox100B (red) in the following genotypes of flies driven by esg-Gal4^{ts} for two days: WT (A and A′), *UAS-upd* (B and B′), *UAS-dome^{DN}* (C and C′), *UAS-Ras^{v12}* (D and D′), *UAS-EGFR-RNAi* (E and E′), *UAS-upd;UAS-EGFR^{RNAi}* (F and F′), and *UAS-dome^{DN};UAS-Ras^{v12}* (G and G′).

(H) Relative fluorescence intensity analysis for anti-Sox100B staining of genotypes of flies as indicated in esg^{ts}>GFP^{+} cells.

(I) Quantitative real-time PCR results of Sox100B mRNA levels of genotypes as indicated. Three independent replicates were carried out for each sample.

(J and K) Midguts expression of GFP (green), stained with DAPI (blue), and anti-Sox100B (red) in the following genotypes of flies driven by Myo1A-Gal4^{ts} for two days: WT, *UAS-upd*, and *UAS-EGFR^{top}* (J). Relative fluorescence intensity analysis for anti-Sox100B staining in Myo1A>GFP^{+} cells (K).

(L) Identification of two enhancer regions (E1 and E2) of *Sox100B* via genomic mapping. E1 shows binding activities by Cic via DamID analysis, E2 contains conserved predicted STAT-binding sites.

(M and N) GFP expression in midguts of the following genotypes of flies combined with *Sox100B-lacZ^{E1}* driven by *esg^{ts}-Gal4* and co-stained with anti-lacZ (white): WT, *UAS-EGFR^{top}*, and *UAS-EGFR^{DN}*. Separated color channels for the insets were enlarged and displayed on the right side (M). Quantification of relative anti-lacZ fluorescence intensity in esg^{ts}>GFP^{+} cells (N).

(O and P) GFP expression in midguts of the following genotypes of flies combined with *Sox100B-lacZ^{E2}* driven by *esg^{ts}-Gal4* and co-stained with anti-lacZ (white): WT, *UAS-hop*, *UAS-Dome^{DN}*, *UAS-EGFR^{top}*, and *UAS-EGFR^{DN}*. Separated color channels for the insets were enlarged and displayed on the right side (O). Quantification of relative lacZ fluorescence intensity in esg^{ts}>GFP^{+} cells (P).

(Q and R) Midguts stained by anti-lacZ (white) in *Sox100B-lacZ$^{E2\text{-}4n1}$*, *Sox100B-lacZ$^{E2\text{-}3n}$*, *Sox100B-lacZ$^{E2\text{-}4n2}$*, *Sox100B-lacZ$^{E2\text{-}4n1,4n2}$*, and transgenic flies. lacZ-channels for the insets were enlarged and displayed on the bottom right (Q). Quantification of relative lacZ fluorescence intensity in esg^{ts}>GFP^{+} cells (R). Note that the lacZ signal disappeared in *Sox100B-lacZ$^{E2\text{-}4n1,4n2}$* mutation flies.

(S) A diagram showing the regulatory nexus of intestinal stress, the JAK/STAT and EGFR signaling pathways, and Sox100B.

Flies were shifted to restrictive temperature for two days before analysis. n is as indicated. Significance was measured with unpaired two-tailed t tests. Mean ± SEM. ns, $p > 0.05$; **$p < 0.01$; ****$p < 0.0001$. Scale bars, 20 μm. See also Figure S4.

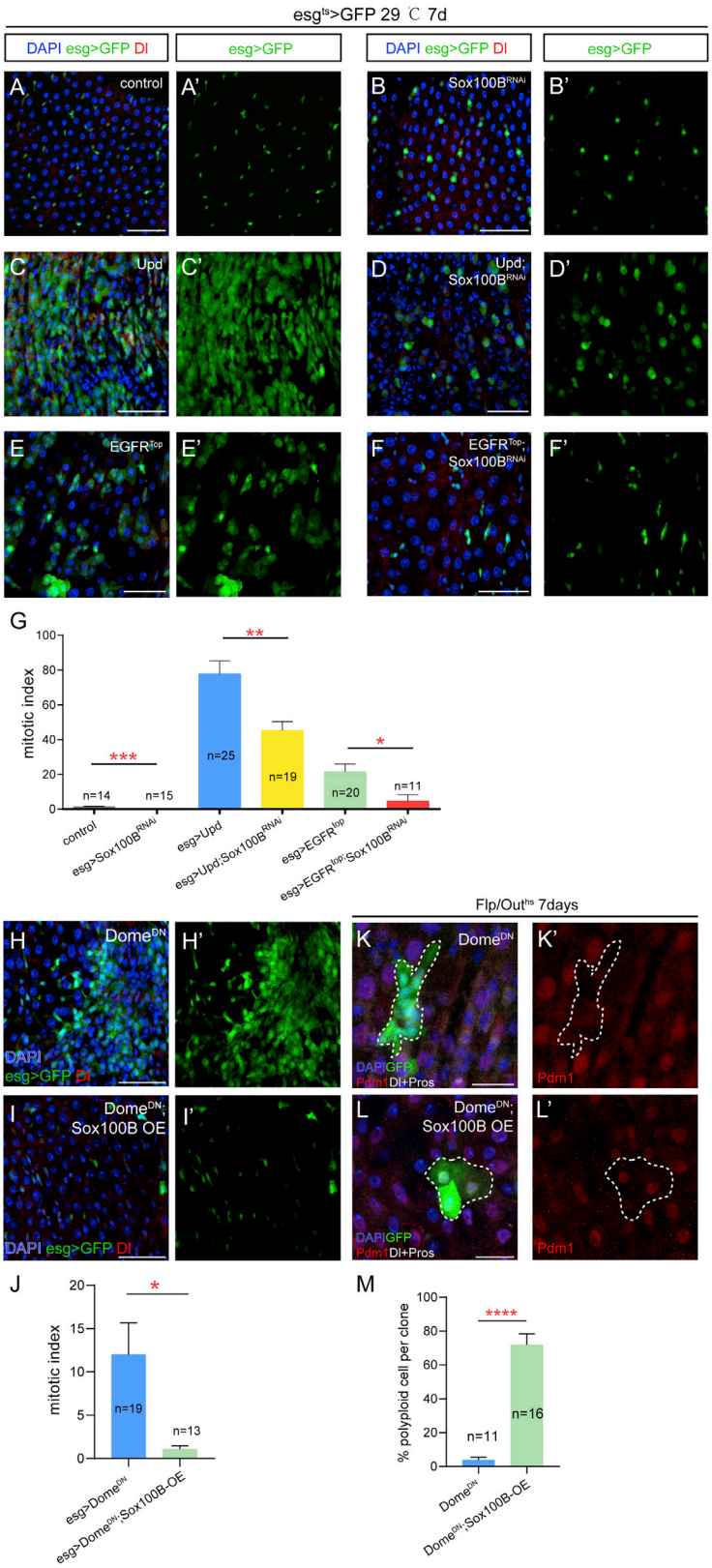

Figure 4. Sox100B Is Required for JAK/STAT- and EGFR Signaling-Activation-Induced ISC Proliferation

(A–F) Midguts of the following genotypes stained with DAPI (blue) and Dl (red): *esg^{ts}>GFP* (A and A′), esg^{ts}>*Sox100B-RNAi* (B and B′), *esg^{ts}>upd* (C and C′), *esg^{ts}>upd;Sox100B-RNAi* (D and D′), *esg^{ts}>EGFR$^{top4.2}$* (E and E′), and *esg^{ts}>EGFR$^{top4.2}$;Sox100B-RNAi* (F and F′).

(G) Mitotic index analysis quantification of PH3^{+} cells for midguts of the following genotypes: *esg^{ts}>GFP*, esg^{ts}>*Sox100B-RNAi*, *esg^{ts}>upd*, *esg^{ts}>upd;Sox100B-RNAi*, *esg^{ts}>EGFR^{top}*, and *esg^{ts}>EGFR^{top};Sox100B-RNAi*.

(H–J) Midguts of the following genotypes stained with DAPI (blue), Dl (red): *esg^{ts}>dome^{DN}* (H and H′), esg^{ts}>*Dome^{DN};Sox100B-OE* (I and I′). Mitotic index analysis via quantification of PH3^{+} cells for midguts of flies as indicated (J).

(K and L) Flp-out clones (marked by GFP, green) with *Dome^{DN}* (K and K′) and *Dome^{DN};Sox100B-OE* (L and L′) overexpression stained with DAPI (blue), anti-Dl (white on membrane), anti-Pros (white in nuclear), anti-Pdm1 (red). Dashed lines depict the clone margin.

(M) Quantification of the percentage of polyploid cells per clone in *Dome^{DN}* or *DomeDN;Sox100B-OE* clones.

Flies were analyzed seven days after being shifted to restrictive temperature or seven days after clone induction. n is as indicated. Significance was measured with unpaired two-tailed t tests. Mean ± SEM. *p < 0.05; **p < 0.01; ***p < 0.001; ****p < 0.0001. Scale bars, 20 μm for (K) and (L), and 50 μm for others.

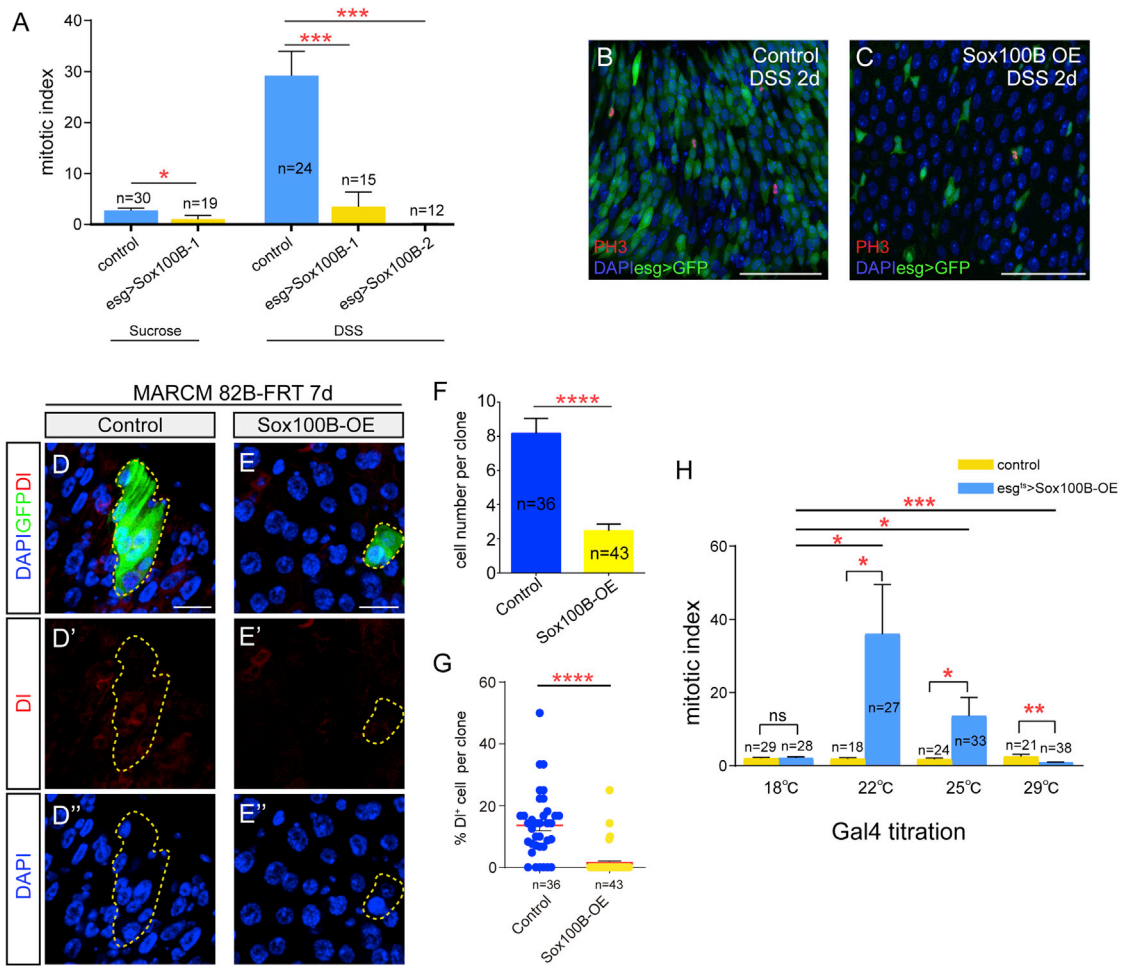

Figure 5. Overexpression of Sox100B Inhibits ISC Proliferation

(A) Mitotic index analysis via quantification of PH3$^+$ cells. Midguts after a two-day sucrose treatment or a two-day DSS treatment were measured.

(B and C) Midguts of the following genotypes of flies stained with DAPI (blue) and anti-PH3 (red): *esg^{ts}>GFP* (B) and *esg^{ts}>Sox100B* (C). Flies were treated with DSS for two days before analysis.

(D and E) MARCM clonal analysis for cell fate changes of ISCs. Analysis was carried out after seven days of clone induction. GFP$^+$ clones co-stained with DAPI (blue) and anti-Dl (red on membrane). (D–D″) A WT *FRT82B* clone. (E–E″) A *Sox100B-overexpressing FRT82B* clone. Dashed lines depict clone margins.

(F) Quantification of the cell number per clone.

(G) Quantification of the proportion of Dl$^+$ cells per clone.

(H) Mitotic index analysis of WT and Sox100B-overexpressed guts driven by temperature titration of esg-Gal4^{ts}. Adult female flies were cultured with the same conditions, except for different temperatures: 18°C, 22°C, 25°C, and 29°C.

n is as indicated. Significance was measured with unpaired two-tailed t tests. Mean ± SEM. $^{ns}p > 0.05$; $^*p < 0.05$; $^{**}p < 0.01$; $^{***}p < 0.001$; $^{****}p < 0.0001$. Scale bars, 50 μm in (B) and (C), and 20 μm in (D) and (E). See also Figures S1, S2, and S3.

We sought to further explore the mechanisms underlying this unusual effect of Sox100B function. We performed comparative gene expression analysis by RNA sequencing (RNA-seq) of wild-type, Sox100B-depleted, and Sox100B-overexpressed intestinal progenitor cells and assessed the potential genomic binding sites of Sox100B using iDam-ID technology (Figures 6A, 6B, S5A, and S5B; Tables S1 and S2; Gutierrez-Triana et al., 2016). Both Sox100B depletion and overexpression caused transcriptional alternations of many genes that are involved in the regulation of cell proliferation, and many of these genes are also identified as Sox100B-iDamID targets (highlighted in bold in Figures S5C and S5D; Tables S1 and S2). Following Sox100B depletion, some positive regulators of cell proliferation are among the significantly downregulated genes, while some negative regulators of cell cycle are among the significantly up-regulated genes. A series of Notch-target genes including *E(spl)mbeta-HLH*, *E(spl)m3-HLH*, and *E(spl)m7-HLH*, were also upregulated upon Sox100B depletion, and our recent study shows that E(spl)-C genes that are expressed in ISCs negatively regulate ISC proliferation (Figures 6A and S5C; Guo et al., 2019).

Following Sox100B overexpression, several cell-cycle/DNA-replication/cell-proliferation-related genes were significantly downregulated (Figure S5D). Interestingly, EGFR was also significantly downregulated (Figure 6A; S5D). Overexpression of

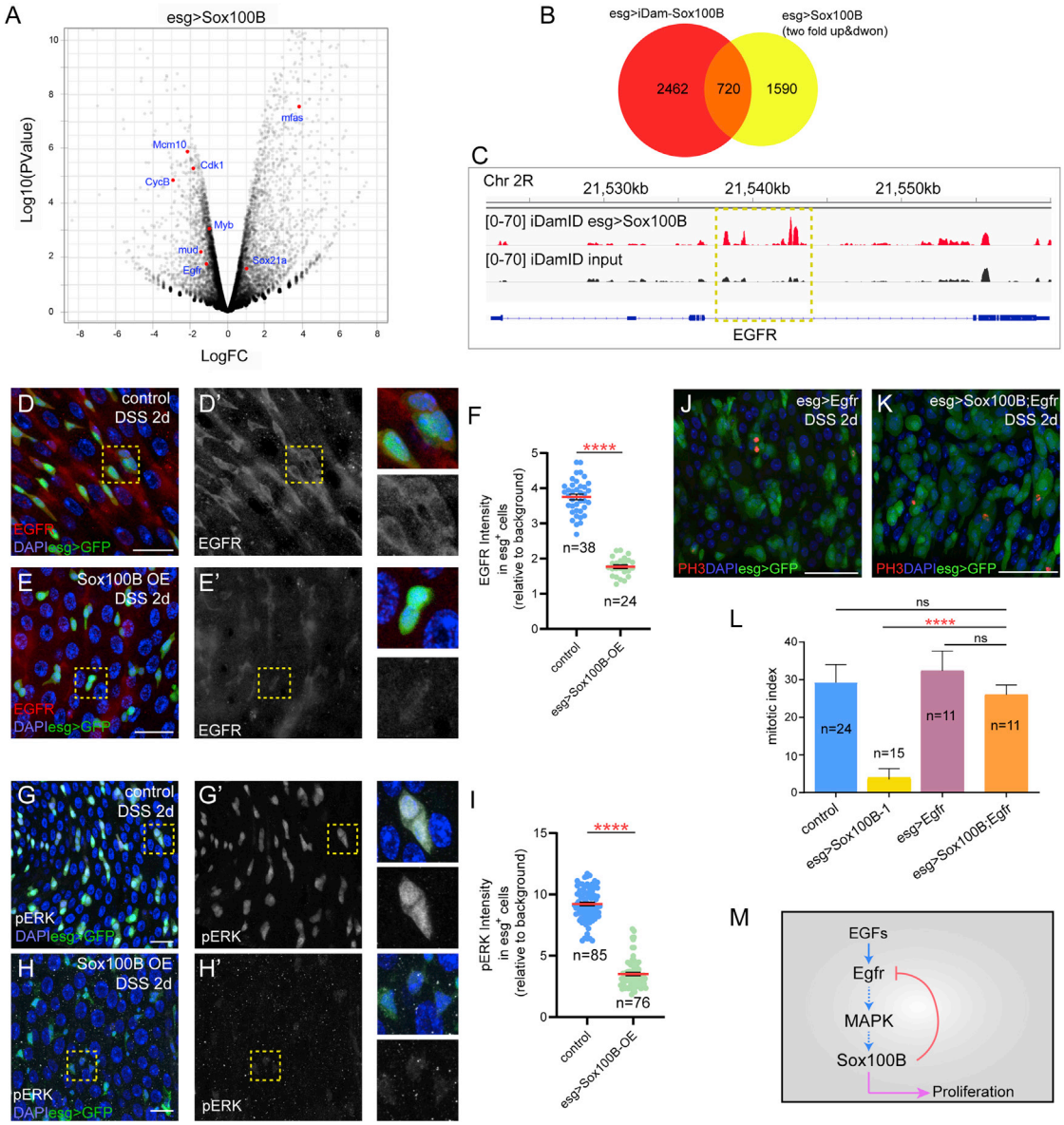

Figure 6. High Level of Sox100B Inhibits ISC Proliferation via a Negative Feedback Mechanism Targeting EGFR

(A) A scatterplot shows the comparison of gene expression profiles of esg^{ts}>GFP^{+} cells in WT and Sox100B-overexpressing midguts. Red dots depict genes with known function on cell proliferation and/or differentiation with 2-fold and higher changes, including decreased genes (left) and increased genes (right). Both WT and Sox100B overexpression datasets have three biological replicates.

(B) A Venn diagram showed the overlap between genes with significant binding activities (two-fold, $p < 0.05$) of Sox100B via iDam-ID analysis (left) and genes altered (two-fold up-/downregulated, $p < 0.05$) upon Sox100B overexpression in progenitor cells via RNA-seq analysis (right).

(C) iDam-ID analysis for Sox100B in progenitor cells revealed binding activities for Sox100B at the genome region of *Egfr*.

(D–F) Midguts of the following genotypes of flies stained with anti-EGFR (red in D and E; white in D′ and E′): *esg^{ts}>GFP* (D and D′) or *esg^{ts}>Sox100B OE* (E and E′). Quantitative analysis for fluorescence intensity of EGFR in esg^{ts}>GFP^{+} cells (F). Separated color channels for the insets were enlarged and displayed on the right side.

(G–I) Midguts of the following genotypes of flies stained with anti-phospho-ERK (pERK, white): *esg^{ts}>GFP* (G and G′) or *esg^{ts}>Sox100B OE* (H and H′). Quantitative analysis for fluorescence intensity of pERK in esg^{ts}>GFP^{+} cells (I). Separated color channels for the insets were enlarged and displayed on the right side.

(J and K) Midguts treated with DSS for two days and stained with anti-PH3 (red) in *esg^{ts}>Egfr* (J), *esg^{ts}>Sox100B;Egfr* (K) female flies.

(L) Mitotic index analysis via quantification of PH3^{+} cells in midguts of the following genotypes: *esg^{ts}>GFP*, *esg^{ts}>Sox100B-1*, *esg^{ts}>Egfr*, *esg^{ts}>Sox100B;Egfr*.

(M) A diagram showing the negative feedback regulation of Sox100B.

Flies (D–L) were treated with DSS for two days before measurements. n is as indicated. Significance was measured with unpaired two-tailed t tests. Mean ± SEM. $^{ns}p > 0.05$; ****$p < 0.0001$. Scale bars, 50 μm in (J) and (K), and 20 μm in others. See also Figure S5 and Tables S1 and S2.

Sox100B also induced expression of a differentiation-related gene *Sox21a* (details will be described later in this article). Notably, genes that were significantly down-/upregulated upon Sox100B depletion showed little alteration upon Sox100B overexpression, and vice versa (Figures S5C and S5D), indicating that different cellular levels of Sox100B result in differential targeting of particular gene subsets, including cell-cycle/cell-proliferation genes. Although the targeted genes are distinct, too high or too low levels of Sox100B both result in an overall negative impact on ISC proliferation. Only within a given dosage-range of Sox100B expression can the proper rate of ISC proliferation proceed, thus affecting a precise control of intestinal regeneration.

One notable observation from the above RNA-seq and DamID results is that EGFR itself is possibly a transcriptional target of Sox100B: overexpression of Sox100B significantly downregulated EGFR expression, and several Sox100B-DamID peaks were found in the genomic region of the EGFR gene (Figure 6C). Staining with anti-EGFR antibody indeed revealed that overexpression of Sox100B caused dramatic reduction of EGFR expression in both normal and stressed conditions (Figures 6D–6F, S5E, and S5F), and not surprisingly, dramatic reduction of phospho-ERK expression, a direct readout of EGFR/Ras/MAPK signaling activity, in progenitor cells as well (Figures 6G–6I, S5E, and S5F). Importantly, overexpression of a *UAS-EGFR* transgene effectively rescued the dampened ISC proliferation response to DSS treatment caused by Sox100B overexpression (Figures 6J–6L). However, depletion of Sox100B had no obvious effect on EGFR level (Figure S5G), suggesting that Sox100B is sufficient to suppress EGFR expression only when it is at high levels. These data suggest that although a low level of Sox100B sustained by EGFR/Ras/MAPK and JAK/STAT signaling is important for ISC proliferation, increased Sox100B levels in turn shut down EGFR/Ras/MAPK signaling via a negative feedback loop by suppressing the transcription of EGFR (Figure 6M).

Sox100B Primes ISCs for Differentiation

We found that Pros$^+$ EEs and Pdm1$^+$ ECs were frequently found in Sox100B-overexpressed-MARCM clones (Figures S6A–S6F), suggesting that overexpression of Sox100B does not cause any obvious abnormalities in terminal cell differentiation. However, when Sox100B was overexpressed in EBs (with the NRE-Gal4), we observed approximately 30% of EB cells have the EC marker Pdm1 expressed, although normally Pdm1 is not expressed in NRE>GFP$^+$ cells (Figures S6G–S6I). Thus, it seems that overexpression of Sox100B causes some EBs to undergo precocious differentiation into ECs.

We speculate that genes that are involved in the differentiation process might be expressed at a relatively low level in progenitor cells but are upregulated to a high level upon differentiation. We thus compared the cell-type-specific transcriptome of ISC, EC, and EE in order to identify genes that are associated with cell differentiation (Dutta et al., 2015). Comparison of ISC and EC transcriptome allowed us to identify 169 EC-enriched genes. As these genes are also expressed at low levels in ISCs, we classify this group of genes as "early-transcribed EC genes." Likewise, by comparing the transcriptome of ISC and EE, we identified 452 EE-enriched genes and classified this group as "early-transcribed EE genes" (Table S3).

Interestingly, we found that a significant portion of early-transcribed EC genes (77 out of 169) and a significant portion of early-transcribed EE genes (142 out of 452) were genes significantly downregulated when Sox100B was knocked down (Figure S6J). Comparatively, a relatively smaller portion of early-transcribed EC or EE genes were upregulated upon Sox100B overexpression (Figure S6K). Many of these early-transcribed genes were also directly targeted by Sox100B (Figure S6L; Table S2). We analyzed these early-transcribed EC/EE genes that are sensitive to Sox100B perturbation by the Gene List Annotation for *Drosophila* (GLAD; Hu et al., 2015). Genes classified as metabolic, transporter, trans-membrane protein, cytoskeletal, receptor, and glycoprotein were found in early-transcribed EC genes; examples include genes encoding digestive enzymes (*stl*, *CG30283*) and immune response factors (*Tep2*) that are linked to EC-specific functions (Figure S6M). Genes classified as secreted protein, GPCR, Mitochondrial, Trans-membrane protein, and lysosomal were found in early-transcribed EE genes; these genes encode hormone peptides (*TK*, *NPF*, *Dh31*, and *Gbp5*) and receptors of *AstA*, *CCHa1*, as well as enzymes and trans-membrane protein as *amon*, *cac*, and *Sytbeta,* that are linked to EE-specific functions (Figure S6N).

These data suggest that a low level of Sox100B promotes the expression of early-transcribed EC/EE genes in ISCs, thereby facilitating ISC differentiation toward functional EC/EE. Depletion of Sox100B caused a failure of differentiation-program activation, and consequently, an arrest in cell differentiation. In contrast, overexpression of Sox100B produces a very mild differentiation phenotype, as overexpression of Sox100B appears to have weak or limited ability to activate early-transcribed EC/EE genes, possibly because in this case Sox100B may need other partners for its transcriptional activity, as partnership with other transcription factors is a common feature of Sox family genes for their transcriptional activity.

A Sox100B-Sox21a-Pdm1 Regulatory Circuitry Promotes Progenitor Cell Differentiation

Previous studies have shown that Sox21a, another Sox family transcription factor, is expressed in intestinal progenitor cells, is upregulated upon differentiation, and is required for terminal differentiation (Chen et al., 2016; Zhai et al., 2017, 2015). In addition, Sox21a bears a striking resemblance to Sox100B in its dynamic expression under stress conditions (Figure 1D). These phenotypic similarities suggest potential functional and regulatory relationships between these two transcription factors. Indeed, our RNA-seq data showed that Sox21a was in the list of significantly upregulated genes upon Sox100B overexpression (Figures 6A and S5D; Table S1). We found that ectopic expression of Sox100B in EBs indeed dramatically increased the expression of Sox21a in EBs (Figures 7A–7E). Conversely, knockdown of Sox100B in EBs reduced Sox21a expression in EBs (Figures 7C–7E). Overexpression or knockdown of Sox100B in ISCs caused similar up- or downregulation of Sox21a, respectively, but the effect is not as striking as that in EBs (Figures S7A–S7C). In addition, knockdown of Sox100B caused failed Sox21a upregulation following DSS-induced intestinal damage

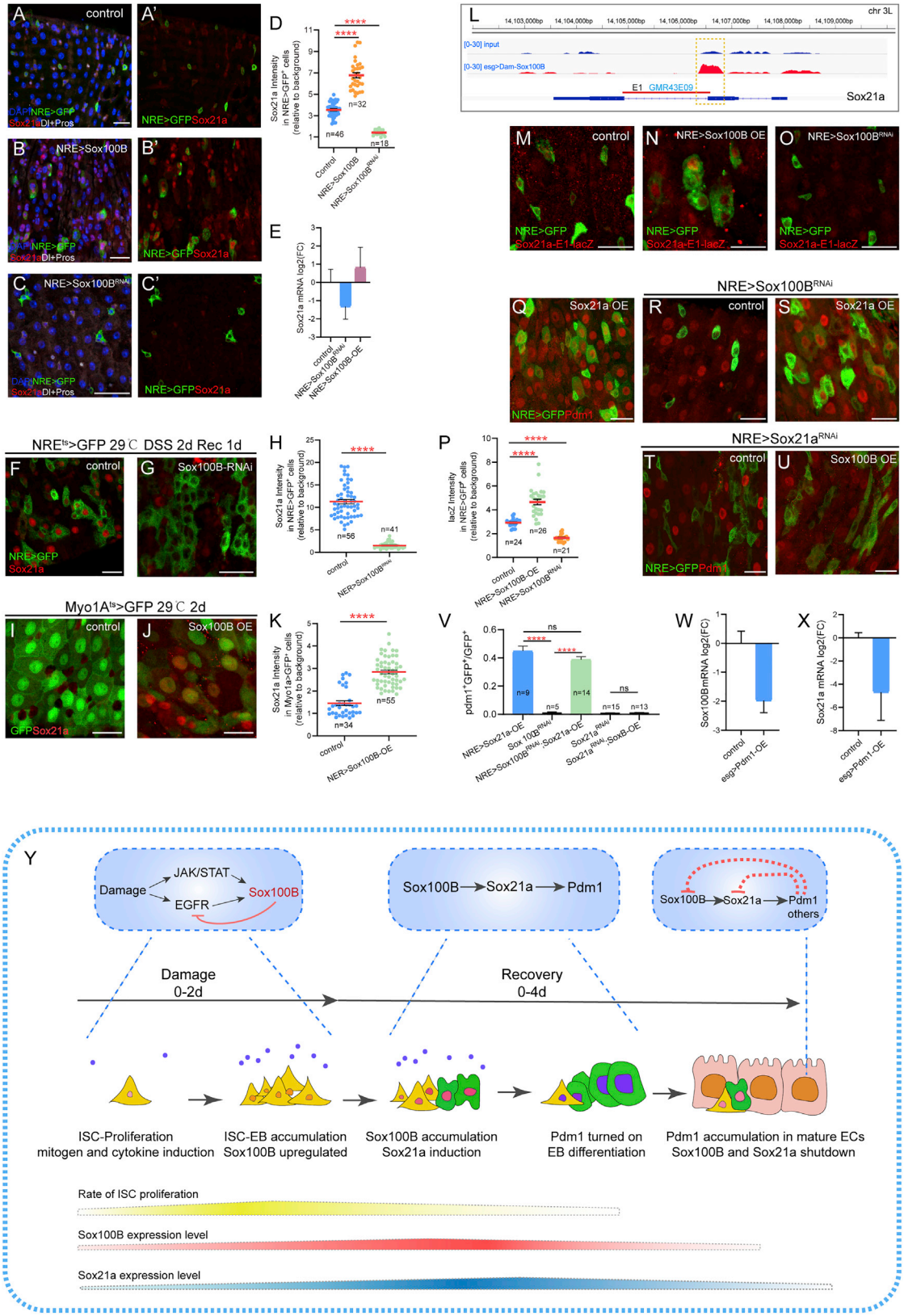

(legend on next page)

(Figures 7F–7H). Furthermore, ectopic expression of Sox100B in ECs induced ectopic Sox21a expression in ECs (Figures 7I–7K). Lastly, overexpression of Sox21a does not have any obvious effect on the expression of Sox100B (not shown). Collectively, these results demonstrate that Sox100B acts upstream to regulate Sox21a expression, but not vice versa.

Interestingly, we found a significant Sox100B-DamID signal peak in the Sox21a genomic region that spans about 4.5k bps from the first to the second intron, and this region partially overlaps with the known gut enhancer element (known as the "E1 element," or GMR43E09 fragment) for Sox21a (Figure 7L). We monitored the transcriptional activity of the Sox21a-E1-lacZ reporter and found that Sox100B overexpression in EBs effectively promoted the expression of lacZ in EBs, whereas Sox100B knockdown effectively diminished LacZ expression in EBs (Figures 7M–7P). These data suggest that Sox100B directly regulates Sox21a expression in progenitor cells.

We found that overexpression of Sox21a in Sox100B-depleted EBs restored the ability for EB to differentiate (Figures 7Q–7S and 7V), as some of these mutant EBs showed Pdm1 expression. However, overexpression of Sox100B in Sox21a-depleted EBs failed to induce cell differentiation (Figures 7T–7V). Therefore, Sox100B functions upstream of Sox21a to promote EB differentiation.

Given that Sox100B and Sox21a are both transiently upregulated in differentiating EBs and diminished in terminally differentiated cells, we hypothesize that there might be a mechanism that inactivates the expression of Sox100B and Sox21a in mature ECs. In light of our earlier finding that Sox100B and Sox21a both upregulate Pdm1, which induces EC differentiation (Korzelius et al., 2014), we tested whether Pdm1 had a counter effect on the expression of Sox100B and Sox21a. Transient overexpression of Pdm1 in progenitor cells for 48 h rapidly shut down Sox100B and Sox21a expression in these cells (Figures 7W, 7X, and S7D–S7I). In addition, Depleting Pdm1 in the differentiated ECs also caused weak appearance of Sox100B expression in some ECs (Figures S7J–S7M). Therefore, it appears that there is also a feedback mechanism in this Sox100B/Sox21a-mediated differentiation process wherein the accumulation of Pdm1, possibly along with other induced factors, can in turn inactivate the expression of Sox100B and Sox21a (Figure 7Y). Conceivably, this feedback mechanism could help to timely terminate the differentiation program and finalize terminal cell differentiation.

DISCUSSION

Sox100B Coordinates Intestinal Homeostasis and Regeneration Downstream of JAK/STAT and EGFR Signaling Pathways

Although it has been well established that in the *Drosophila* midgut, the stress-responsive JAK/STAT signaling and EGFR/Ras/MAPK signaling are the two major signaling pathways that regulate ISC proliferation and differentiation, the downstream signaling targets that coordinate ISC proliferation and differentiation for intestinal regeneration are still yet to be identified. Sox100B identified in this study may represent such a key target. First, the expression of Sox100B is regulated by both JAK/STAT- and EGFR-signaling pathways. Normally Sox100B is expressed specifically in ISCs and EBs, where JAK/STAT- and EGFR/Ras/MAPK-pathway activities are high, and its expression is highly dependent on the activity of JAK/STAT- and EGFR/Ras/MAPK-signaling activities. Second, similar to the functions of JAK/STAT and EGFR signaling, Sox100B is critically required for both ISC proliferation and differentiation. The sustained EGFR/Ras/MAPK activity in EBs is important for the initiation

Figure 7. A Sox100B-Sox21a-Pdm1 Regulatory Circuitry Drives Cell Differentiation

(A–C) Midguts expression of GFP (green) and co-stained with DAPI (blue), anti-Sox21a (red), anti-Dl (white on membrane), and anti-Pros (white in nuclear) in the following genotypes of flies: *NRE^{ts}>GFP* (A and A′), *NRE^{ts}>Sox100B* (B and B′), and *NRE^{ts}>Sox100B-RNAi* (C and C′).

(D) Quantitative analysis for fluorescence intensity of anti-Sox21a staining in NRE^{ts}>GFP^{+} cells in WT, *NRE^{ts}>Sox100B*, and *NRE^{ts}>Sox100B-RNAi* midguts.

(E) Quantitative real-time PCR results of Sox21a mRNA levels for WT, *NRE^{ts}>Sox100B* and *NRE^{ts}>Sox100B-RNAi* midguts. Three independent replicates were carried out for each sample.

(F–H) GFP expression and co-stained with anti-Sox21a (red) in midguts of the following genotypes of flies: *NRE^{ts}>GFP* (F) and *NRE^{ts}>Sox100B-RNAi* (G). Quantification of relative Sox21a fluorescence intensity in NRE>GFP+ cells (H). Flies were shifted to restrictive temperature and fed for DSS for two days, then to recovery for one day before analysis.

(I–K) GFP expression and co-stained with anti-Sox21a (red) in midguts of the following genotypes: *Myo1A^{ts}>GFP* (I) and *Myo1A^{ts}>Sox100B* (J). Quantitative analysis of relative Sox21a fluorescence intensity in Myo1A>GFP+ cells (K).

(L) iDam-ID analysis for *Sox100B* in progenitor cells revealed binding activities for *Sox100B* at the genome region (GMR43E09, E1 enhancer) of *Sox21a*.

(M–P) GFP expression and co-stained with anti-lacZ (red, GMR43E09-lacZ) in midguts of the following genotypes: *NRE^{ts}>GFP* (M), *NRE^{ts}>Sox100B* (N), and *NRE^{ts}>Sox100B-RNAi* (O). Quantification of relative lacZ fluorescence intensity in NRE^{ts}>GFP+ cells (P).

(Q–U) Midguts expression of GFP and co-stained with anti-Pdm1 (red) in *NRE^{ts}>Sox21a* (Q), *NRE^{ts}>Sox100B-RNAi* (R), *NRE^{ts}>Sox100B-RNAi;Sox21a* (S), *NRE^{ts}>Sox21a-RNAi* (T), and *NRE^{ts}>Sox100B;Sox21a-RNAi* (U) flies.

(V) Quantification about percentages of GFP^{+}Pdm1^{+}/GFP^{+} cells per frame (every 3 x 10^{4} μm^{2}) for genotypes as indicated.

(W and X) Quantitative real-time PCR results of Sox100B mRNA levels (W) and Sox21a mRNA levels (X) for WT and progenitor-specific Pdm1 overexpressed midguts. Three independent replicates were carried out for each sample.

(Y) A schematic model: Sox100B as a homeostatic sensor and coordinator in intestinal homeostasis and regeneration in *Drosophila*. ISC activity is responsive to epithelial damage via stress-responsive JAK/STAT and EGFR signaling pathways, both of which directly regulate Sox100B transcription via separate enhancers. Although Sox100B is essential for ISC proliferation, the upregulated Sox100B following damage in turn (1) inhibits EGFR expression to shut down cell proliferation, and (2) activates cell differentiation via a differentiation-promoting circuit composed of Sox100B, Sox21a, and Pdm1, thereby providing a feedback mechanism to promote the transition from cell proliferation to differentiation for rapid epithelial repair and homeostasis re-establishment.

Flies were shifted to restrictive temperature for seven days (in Q–V) or two days (others) before analysis. n is as indicated. Significance was measured with unpaired two-tailed t tests. Mean ± SEM. ns, $p > 0.05$; ****$p < 0.0001$. Scale bars, 20 μm.

See also Figures S6 and S7 and Table S3.

of DNA endoreplication during the process of EC differentiation (Xiang et al., 2017), and the sustained JAK/STAT signaling activity in EBs is essential for terminal differentiation toward both EC and EE lineages (Beebe et al., 2010; Jiang et al., 2009; Lin et al., 2010). Depletion of Sox100B causes ISC quiescence, similar to that caused by the disruption of EGFR signaling, as well as arrest of EB differentiation, similar to that caused by the disruption of JAK/STAT signaling. Third, an appropriate level of Sox100B expression appears to be critical for intestinal homeostasis. This effect by the expression level, as well as its responsiveness to JAK/STAT, EGFR, and potentially other stress-induced signaling activities (not shown), such as Wnt and Hippo signaling (Cordero et al., 2012b; Karpowicz et al., 2010; Ren et al., 2010; Shaw et al., 2010), may position Sox100B as a central mediator that coordinates ISC proliferation and differentiation during intestinal homeostasis and regeneration in *Drosophila*.

Sox Transcription Factors with a "Dosage Effect"

Sox100B is a Sox family group-E transcription factor, homolog of mammalian Sox8/9/10. In mouse small intestine, Sox9 is expressed in stem cells and progenitor cells at the base of crypts, and loss of Sox9 in the intestinal epithelium causes ISC hyperplasia and failure of Paneth cell differentiation (Bastide et al., 2007; Mori-Akiyama et al., 2007). Interestingly, in the stem cell zone, Sox9 is expressed at low levels in ISCs and high levels in the quiescent or reserved stem cells that are also considered as the secretory progenitors (Formeister et al., 2009; Roche et al., 2015). A possible explanation for these observations is that a low level of Sox9 sustains actively dividing ISCs, while an increase of SOX9 converts these proliferating ISCs into quiescent ISCs that will eventually differentiate into Paneth cells. Similarly, Sox9 is also implicated in regulating colorectal cancer cells, but there are conflicting data regarding whether Sox9 functions as an oncogene or a tumor suppressor (Prévostel and Blache, 2017). These seemingly contradictory results can be reconciled with a proposed model that Sox9 functions at an appropriate level, with a critical dose of Sox9 that exhibits proliferation-promoting activity, while increasing or decreasing this dose both result in proliferation-inhibitory activity (Prévostel and Blache, 2017). It is worthy to note that the differentiation-promoting function of Sox9 could potentially further complicate the interpretation of the mutant phenotype. It has been shown in *Drosophila* gut that defects in differentiation can induce a stressed microenvironment that promotes cell proliferation and propels tumor development (Patel et al., 2015; Zhai et al., 2015).

Our results here suggest many aspects of functional conservation of this Sox E subfamily gene in ISCs from *Drosophila* to mammals. Sox100B regulates both ISC proliferation and differentiation in the *Drosophila* intestine, and in terms of regulating ISC proliferation, Sox100B also requires an appropriate expression level. Here we have demonstrated that this modulation of Sox100B expression is largely due to a negative feedback mechanism, in which increased Sox100B caused by elevated EGFR/Ras/MAPK signaling in turn suppresses the expression of EGFR, thereby leading to damped EGFR-signaling activity. Of note, contradictory data were recently reported on the roles of Sox100B and Sox21a in regulating ISC proliferation: both a proliferation-promoting role (Meng and Biteau, 2015) and a tumor-suppressive role (Chen et al., 2016; Zhai et al., 2015) for Sox21a in ISCs have been reported; as for the role of Sox100B, Lan et al. (2018) showed in an RNAi genetic screen that Sox100B is required for P.e.-induced ISC proliferation, whereas Doupé et al. (2018) showed that depletion of Sox100B by RNAi causes increased ISC proliferation. Consideration of the effects caused by different levels of Sox100B expression that we observed in the present study may help resolve our understanding of apparently disparate functions for these genes as central coordinators of both ISC proliferation and differentiation. We propose that, normally, a low level of Sox protein expression sustains ISC proliferation. A transient increase of Sox protein may not only promote cell cycle exit but also activate programs for terminal differentiation, thereby leading to a coordinated ISC proliferation and differentiation and, consequently, a coherent process of epithelial renewal.

A Sox100B-Sox21a-Pdm1 Regulatory Pathway in Promoting EC Differentiation

Our study demonstrates that Sox100B directly regulates Sox21a to promote differentiation. One important downstream target of Sox100B and Sox21a appears to be Pdm1, a known EC-fate-promoting factor (Korzelius et al., 2014; Tang et al., 2018). Interestingly, overexpression of Pdm1 in progenitor cells rapidly shuts down both Sox100B and Sox21a expression, indicating a negative feedback mechanism. Therefore, the induced Sox100B-Sox21a-Pdm1 axis in the differentiating ECs not only promotes cell differentiation, but also acts in a feedback mechanism to turn down EGFR and JAK/STAT signaling activities, thereby allowing ECs to terminally differentiate. This differentiation-promoting axis might also have a role in turning down ISC-specific programs, which are independently regulated by EGFR or JAK/STAT signaling pathways. For example, downregulation of the stem-cell-factor Esg is required for EB differentiation (Korzelius et al., 2014; Loza-Coll et al., 2014), and ectopic expression of Pdm1 is able to antagonize Esg expression in progenitor cells (Korzelius et al., 2014). These kinds of feedback regulation could be a common strategy used for initiation and finalization of a cell-differentiation program.

In summary, our study identified the transcription factor Sox100B as a major effector downstream of JAK/STAT and EGFR pathways that acts at an appropriate level to coordinate ISC proliferation and differentiation during both normal intestinal homeostasis and during damage- and infection-induced intestinal regeneration in *Drosophila*. With the "just-right" effect endowed by a feedback mechanism, Sox100B behaves as a homeostatic sensor in the intestinal epithelium that coordinates stem cell proliferation with stem cell differentiation under various environmental conditions. We propose that this expressional and functional modulation associated with Sox family transcription factors may be a general mechanism for maintaining tissue homeostasis and regeneration in many organs, including those in mammals, and that deregulation of this mechanism may lead to tissue degeneration or cancer development.

STAR★METHODS

Detailed methods are provided in the online version of this paper and include the following:

SUPPLEMENTAL INFORMATION

Supplemental Information can be found online at https://doi.org/10.1016/j.celrep.2020.107683.

ACKNOWLEDGMENTS

We thank the fly community as cited in the Key Resources Table for generously providing fly stocks, antibodies, and/or other materials; the Bloomington Drosophila Stock Center (BDSC); the Tsinghua Fly Center; the Vienna Drosophila RNAi Center (VDRC); the National Institute of Genetics (NIG); the Drosophila Genomics Resource Center (DGRC); the Developmental Studies Hybridoma Bank (DSHB) for fly stocks and reagents; and NIBS Antibody Center for generating the Sox100B antisera. This work was supported by the National Key Research and Development Program of China (2017YFA0103602) and the National Basic Research Program of China (2014CB850002) from the Chinese Ministry of Science and Technology. J.C. is supported by the Initiative Postdocs Supporting Program of China (214394).

AUTHOR CONTRIBUTIONS

Conceptualization, Z.J. and R.X.; Methodology, Z.J. and R.X.; Investigation, Z.J., J.C., J.L., M.Y., and X.G.; Software and Formal Analysis, H.H., J.W., Y.Z., and T.C.; Writing — Original Draft, Z.J. and R.X.; Writing — Review & Editing, Z.J. and R.X.; Funding Acquisition, R.X.; Supervision, R.X.

DECLARATION OF INTERESTS

The authors declare no competing interests.

Received: October 14, 2019
Revised: March 13, 2020
Accepted: May 2, 2020
Published: May 26, 2020

REFERENCES

Amcheslavsky, A., Jiang, J., and Ip, Y.T. (2009). Tissue damage-induced intestinal stem cell division in Drosophila. Cell Stem Cell *4*, 49–61.

Amcheslavsky, A., Nie, Y., Li, Q., He, F., Tsuda, L., Markstein, M., and Ip, Y.T. (2014). Gene expression profiling identifies the zinc-finger protein Charlatan as a regulator of intestinal stem cells in Drosophila. Development *141*, 2621–2632.

Bastide, P., Darido, C., Pannequin, J., Kist, R., Robine, S., Marty-Double, C., Bibeau, F., Scherer, G., Joubert, D., Hollande, F., et al. (2007). Sox9 regulates cell proliferation and is required for Paneth cell differentiation in the intestinal epithelium. J. Cell Biol. *178*, 635–648.

Beebe, K., Lee, W.C., and Micchelli, C.A. (2010). JAK/STAT signaling coordinates stem cell proliferation and multilineage differentiation in the Drosophila intestinal stem cell lineage. Dev. Biol. *338*, 28–37.

Biteau, B., and Jasper, H. (2011). EGF signaling regulates the proliferation of intestinal stem cells in Drosophila. Development *138*, 1045–1055.

Biteau, B., Hochmuth, C.E., and Jasper, H. (2008). JNK activity in somatic stem cells causes loss of tissue homeostasis in the aging Drosophila gut. Cell Stem Cell *3*, 442–455.

Biteau, B., Hochmuth, C.E., and Jasper, H. (2011). Maintaining tissue homeostasis: dynamic control of somatic stem cell activity. Cell Stem Cell *9*, 402–411.

Brand, A.H., and Perrimon, N. (1993). Targeted gene expression as a means of altering cell fates and generating dominant phenotypes. Development *118*, 401–415.

Brown, S., Hu, N., and Hombría, J.C. (2001). Identification of the first invertebrate interleukin JAK/STAT receptor, the Drosophila gene Domeless. Curr. Biol. *11*, 1700–1705.

Buchon, N., Broderick, N.A., Chakrabarti, S., and Lemaitre, B. (2009a). Invasive and indigenous microbiota impact intestinal stem cell activity through multiple pathways in Drosophila. Genes Dev. *23*, 2333–2344.

Buchon, N., Broderick, N.A., Poidevin, M., Pradervand, S., and Lemaitre, B. (2009b). Drosophila intestinal response to bacterial infection: activation of host defense and stem cell proliferation. Cell Host Microbe *5*, 200–211.

Buchon, N., Broderick, N.A., Kuraishi, T., and Lemaitre, B. (2010). Drosophila EGFR pathway coordinates stem cell proliferation and gut remodeling following infection. BMC Biol. *8*, 152.

Chen, J., Xu, N., Huang, H., Cai, T., and Xi, R. (2016). A feedback amplification loop between stem cells and their progeny promotes tissue regeneration and tumorigenesis. eLife *5*, e14330.

Chen, J., Xu, N., Wang, C., Huang, P., Huang, H., Jin, Z., Yu, Z., Cai, T., Jiao, R., and Xi, R. (2018). Transient scute activation via a self-stimulatory loop directs enteroendocrine cell pair specification from self-renewing intestinal stem cells. Nat. Cell Biol. *20*, 152–161.

Cordero, J.B., Stefanatos, R.K., Myant, K., Vidal, M., and Sansom, O.J. (2012a). Non-autonomous crosstalk between the JAK/STAT and EGFR pathways mediates Apc1-driven intestinal stem cell hyperplasia in the Drosophila adult midgut. Development *139*, 4524–4535.

Cordero, J.B., Stefanatos, R.K., Scopelliti, A., Vidal, M., and Sansom, O.J. (2012b). Inducible progenitor-derived Wingless regulates adult midgut regeneration in Drosophila. EMBO J. *31*, 3901–3917.

Doupé, D.P., Marshall, O.J., Dayton, H., Brand, A.H., and Perrimon, N. (2018). *Drosophila* intestinal stem and progenitor cells are major sources and regulators of homeostatic niche signals. Proc. Natl. Acad. Sci. USA *115*, 12218–12223.

Dutta, D., Xiang, J., and Edgar, B.A. (2013). RNA expression profiling from FACS-isolated cells of the Drosophila intestine. Curr. Protoc. Stem Cell Biol. *27*, Unit 2F, 2.

Dutta, D., Dobson, A.J., Houtz, P.L., Gläßer, C., Revah, J., Korzelius, J., Patel, P.H., Edgar, B.A., and Buchon, N. (2015). Regional cell-specific transcriptome mapping reveals regulatory complexity in the adult Drosophila midgut. Cell Rep. *12*, 346–358.

Formeister, E.J., Sionas, A.L., Lorance, D.K., Barkley, C.L., Lee, G.H., and Magness, S.T. (2009). Distinct SOX9 levels differentially mark stem/progenitor populations and enteroendocrine cells of the small intestine epithelium. Am. J. Physiol. Gastrointest. Liver Physiol. *296*, G1108–G1118.

Freeman, M. (1996). Reiterative use of the EGF receptor triggers differentiation of all cell types in the Drosophila eye. Cell *87*, 651–660.

Goto, S., and Hayashi, S. (1999). Proximal to distal cell communication in the Drosophila leg provides a basis for an intercalary mechanism of limb patterning. Development *126*, 3407–3413.

Guo, X., Huang, H., Yang, Z., Cai, T., and Xi, R. (2019). Division of labor: roles of Groucho and CtBP in Notch-mediated lateral inhibition that controls intestinal stem cell differentiation in Drosophila. Stem Cell Reports *12*, 1007–1023.

Gutierrez-Triana, J.A., Mateo, J.L., Ibberson, D., Ryu, S., and Wittbrodt, J. (2016). iDamIDseq and iDEAR: an improved method and computational pipeline to profile chromatin-binding proteins. Development *143*, 4272–4278.

Harrison, D.A., Binari, R., Nahreini, T.S., Gilman, M., and Perrimon, N. (1995). Activation of a Drosophila Janus kinase (JAK) causes hematopoietic neoplasia and developmental defects. EMBO J. *14*, 2857–2865.

Hu, Y., Comjean, A., Perkins, L.A., Perrimon, N., and Mohr, S.E. (2015). GLAD: an online database of Gene List Annotation for Drosophila. J Genomics *3*, 75–81.

Jiang, H., and Edgar, B.A. (2011). Intestinal stem cells in the adult Drosophila midgut. Exp. Cell Res. *317*, 2780–2788.

Jiang, H., Patel, P.H., Kohlmaier, A., Grenley, M.O., McEwen, D.G., and Edgar, B.A. (2009). Cytokine/JAK/STAT signaling mediates regeneration and homeostasis in the Drosophila midgut. Cell *137*, 1343–1355.

Jiang, H., Grenley, M.O., Bravo, M.J., Blumhagen, R.Z., and Edgar, B.A. (2011). EGFR/Ras/MAPK signaling mediates adult midgut epithelial homeostasis and regeneration in Drosophila. Cell Stem Cell *8*, 84–95.

Jin, Y., Ha, N., Forés, M., Xiang, J., Gläßer, C., Maldera, J., Jiménez, G., and Edgar, B.A. (2015). EGFR/Ras signaling controls Drosophila intestinal stem cell proliferation via Capicua-regulated genes. PLoS Genet. *11*, e1005634.

Kamachi, Y., and Kondoh, H. (2013). Sox proteins: regulators of cell fate specification and differentiation. Development *140*, 4129–4144.

Karpowicz, P., Perez, J., and Perrimon, N. (2010). The Hippo tumor suppressor pathway regulates intestinal stem cell regeneration. Development *137*, 4135–4145.

Kondo, S., and Ueda, R. (2013). Highly improved gene targeting by germline-specific Cas9 expression in Drosophila. Genetics *195*, 715–721.

Korzelius, J., Naumann, S.K., Loza-Coll, M.A., Chan, J.S., Dutta, D., Oberheim, J., Gläßer, C., Southall, T.D., Brand, A.H., Jones, D.L., and Edgar, B.A. (2014). Escargot maintains stemness and suppresses differentiation in Drosophila intestinal stem cells. EMBO J. *33*, 2967–2982.

Kudron, M.M., Victorsen, A., Gevirtzman, L., Hillier, L.W., Fisher, W.W., Vafeados, D., Kirkey, M., Hammonds, A.S., Gersch, J., Ammouri, H., et al. (2018). The modern resource: genome-wide binding profiles for hundreds of *Drosophila* and *Caenorhabditis elegans* transcription factors. Genetics *208*, 937–949.

Lan, Q., Cao, M., Kollipara, R.K., Rosa, J.B., Kittler, R., and Jiang, H. (2018). FoxA transcription factor Fork head maintains the intestinal stem/progenitor cell identities in Drosophila. Dev. Biol. *433*, 324–343.

Lee, T., and Luo, L. (1999). Mosaic analysis with a repressible cell marker for studies of gene function in neuronal morphogenesis. Neuron *22*, 451–461.

Li, Z., Guo, X., Huang, H., Wang, C., Yang, F., Zhang, Y., Wang, J., Han, L., Jin, Z., and Cai, T. (2020). A switch in tissue stem cell identity causes neuroendocrine tumors in Drosophila gut. Cell Rep. *30*, 1724–1734 e1724.

Liang, J., Balachandra, S., Ngo, S., and O'Brien, L.E. (2017). Feedback regulation of steady-state epithelial turnover and organ size. Nature *548*, 588–591.

Lin, G., Xu, N., and Xi, R. (2008). Paracrine Wingless signalling controls self-renewal of Drosophila intestinal stem cells. Nature *455*, 1119–1123.

Lin, G., Xu, N., and Xi, R. (2010). Paracrine unpaired signaling through the JAK/STAT pathway controls self-renewal and lineage differentiation of Drosophila intestinal stem cells. J. Mol. Cell Biol. *2*, 37–49.

Loza-Coll, M.A., Southall, T.D., Sandall, S.L., Brand, A.H., and Jones, D.L. (2014). Regulation of Drosophila intestinal stem cell maintenance and differentiation by the transcription factor Escargot. EMBO J. *33*, 2983–2996.

Luo, T.L.L. (1999). Mosaic analysis with a repressible neurotechnique cell marker for studies of gene function in neuronal morphogenesis. Neuron *1999*, 451–461.

McGuire, S.E., Mao, Z., and Davis, R.L. (2004). Spatiotemporal gene expression targeting with the TARGET and gene-switch systems in Drosophila. Sci. STKE *2004*, pl6.

Meng, F.W., and Biteau, B. (2015). A SOX transcription factor is a critical regulator of adult stem cell proliferation in the Drosophila intestine. Cell Rep. *13*, 906–914.

Micchelli, C.A., and Perrimon, N. (2006). Evidence that stem cells reside in the adult Drosophila midgut epithelium. Nature *439*, 475–479.

Mori-Akiyama, Y., van den Born, M., van Es, J.H., Hamilton, S.R., Adams, H.P., Zhang, J., Clevers, H., and de Crombrugghe, B. (2007). SOX9 is required for the differentiation of Paneth cells in the intestinal epithelium. Gastroenterology *133*, 539–546.

Ohlstein, B., and Spradling, A. (2006). The adult Drosophila posterior midgut is maintained by pluripotent stem cells. Nature *439*, 470–474.

Ohlstein, B., and Spradling, A. (2007). Multipotent Drosophila intestinal stem cells specify daughter cell fates by differential notch signaling. Science *315*, 988–992.

Patel, P.H., Dutta, D., and Edgar, B.A. (2015). Niche appropriation by Drosophila intestinal stem cell tumours. Nat. Cell Biol. *17*, 1182–1192.

Prévostel, C., and Blache, P. (2017). The dose-dependent effect of SOX9 and its incidence in colorectal cancer. Eur. J. Cancer *86*, 150–157.

Queenan, A.M., Ghabrial, A., and Schüpbach, T. (1997). Ectopic activation of torpedo/EGFR, a Drosophila receptor tyrosine kinase, dorsalizes both the eggshell and the embryo. Development *124*, 3871–3880.

Ren, F., Wang, B., Yue, T., Yun, E.Y., Ip, Y.T., and Jiang, J. (2010). Hippo signaling regulates Drosophila intestine stem cell proliferation through multiple pathways. Proc. Natl. Acad. Sci. USA *107*, 21064–21069.

Roche, K.C., Gracz, A.D., Liu, X.F., Newton, V., Akiyama, H., and Magness, S.T. (2015). SOX9 maintains reserve stem cells and preserves radioresistance in mouse small intestine. Gastroenterology *149*, 1553–1563 e1510.

Sarkar, A., and Hochedlinger, K. (2013). The sox family of transcription factors: versatile regulators of stem and progenitor cell fate. Cell Stem Cell *12*, 15–30.

Shaw, R.L., Kohlmaier, A., Polesello, C., Veelken, C., Edgar, B.A., and Tapon, N. (2010). The Hippo pathway regulates intestinal stem cell proliferation during Drosophila adult midgut regeneration. Development *137*, 4147–4158.

Struhl, G., and Basler, K. (1993). Organizing activity of wingless protein in Drosophila. Cell *72*, 527–540.

Tang, X., Zhao, Y., Buchon, N., and Engström, Y. (2018). The POU/OCT transcription factor Nubbin controls the balance of intestinal stem cell maintenance and differentiation by isoform-specific regulation. Stem Cell Reports *10*, 1565–1578.

Vodovar, N., Vinals, M., Liehl, P., Basset, A., Degrouard, J., Spellman, P., Boccard, F., and Lemaitre, B. (2005). Drosophila host defense after oral infection by an entomopathogenic Pseudomonas species. Proc. Natl. Acad. Sci. USA *102*, 11414–11419.

Xiang, J., Bandura, J., Zhang, P., Jin, Y., Reuter, H., and Edgar, B.A. (2017). EGFR-dependent TOR-independent endocycles support Drosophila gut epithelial regeneration. Nat. Commun. *8*, 15125.

Xu, N., Wang, S.Q., Tan, D., Gao, Y., Lin, G., and Xi, R. (2011). EGFR, Wingless and JAK/STAT signaling cooperatively maintain Drosophila intestinal stem cells. Dev. Biol. *354*, 31–43.

Zeng, X., Chauhan, C., and Hou, S.X. (2010). Characterization of midgut stem cell- and enteroblast-specific Gal4 lines in Drosophila. Genesis *48*, 607–611.

Zhai, Z., Kondo, S., Ha, N., Boquete, J.P., Brunner, M., Ueda, R., and Lemaitre, B. (2015). Accumulation of differentiating intestinal stem cell progenies drives tumorigenesis. Nat. Commun. *6*, 10219.

Zhai, Z., Boquete, J.P., and Lemaitre, B. (2017). A genetic framework controlling the differentiation of intestinal stem cells during regeneration in Drosophila. PLoS Genet. *13*, e1006854.

Zielke, N., Korzelius, J., van Straaten, M., Bender, K., Schuhknecht, G.F.P., Dutta, D., Xiang, J., and Edgar, B.A. (2014). Fly-FUCCI: a versatile tool for studying cell proliferation in complex tissues. Cell Rep. *7*, 588–598.

STAR★METHODS

KEY RESOURCES TABLE

REAGENT or RESOURCE	SOURCE	IDENTIFIER
Antibodies		
Mouse monoclonal anti-Dl	The Developmental Studies Hybridoma Bank	Cat#C594.9B; RRID:AB_528194
Mouse monoclonal anti-Pros	The Developmental Studies Hybridoma Bank	Cat#MR1A; RRID:AB_528440
Rabbit polyclonal anti-Pros	gift from Yuh-Nung Jan, UCSF, USA	N/A
Rabbit polyclonal anti-phospho-Histone H3	Cell Signaling Technology	Cat# 9701; RRID:AB_331535
Rabbit polyclonal anti-Pdm1	gift from Xiaohang Yang, Zhejiang University, China	N/A
Rabbit monoclonal anti-GFP	Cell Signaling Technology	Cat #2956; RRID:AB_1196615
Rabbit polyclonal anti-β-galactosidase	MP Biomedicals	Cat# 0855976, RRID:AB_2334934
Goat polyclonal anti-EGFR	Santa Cruz Biotechnology	Cat# sc-15827; RRID:AB_640059
Rabbit polyclonal anti-phospho-ERK	Cell Signaling Technology	Cat# 4370; RRID:AB_2315112
Mouse polyclonal anti-β-galactosidase	The Developmental Studies Hybridoma Bank	Cat#40-1a
Rabbit monoclonal anti-Cleaved Dcp-1(Asp216)	Cell Signaling	Cat#9578; RRID: AB_2721060
Rabbit polyclonal anti-Sox100B	This paper	N/A
Rabbit polyclonal anti-Sox21a	Chen et al., 2016	N/A
Chemicals, Peptides, and Recombinant Proteins		
DAPI	ThermoFisher	Cat#D1306; RRID:AB_2629482
DSS	MP Biomedicals	Cat#160110
Elastase	Sigma	Cat#: E0258
propidium iodide (PI)	Invitrogen	Cat#: P3566
Peptides used to generate polyclonal antibody against Sox100B: CEQQHQNPSQHHLWGTYTYVN	This paper	N/A
Critical Commercial Assays		
Arcturus PicoPureTM RNA isolation kit	ThermoFisher	Cat#KIT0204
ArcturusTM RiboAmpTM HS PLUS RNA amplification kit	ThermoFisher	Cat# KIT0525
Deposited Data		
Raw and analyzed data: RNA-sequencing	This paper	GEO:GSE130305
Raw and analyzed data: Sox100B DamID-sequencing	This paper	GEO:GSE130305
Experimental Models: Organisms/Strains		
Sox100B-GFP	Bloomington Drosophila Stock Center	BDSC: 66743 Flybase: FBst0066743
UAS-Sox100B-RNAi	Fly Stocks of National Institute of Genetics	NIG:15552R-2
UAS-Sox100B-RNAi	Vienna Drosophila Resource Center	VDRC:45962 Flybase: FBst0466448
UAS-Sox100B-RNAi	Bloomington Drosophila Stock Center	BDSC:35656 Flybase:FBst0035656

(*Continued on next page*)

Continued

REAGENT or RESOURCE	SOURCE	IDENTIFIER
UAS-EGFR-RNAi	Bloomington Drosophila Stock Center	BDSC: 25781 Flybase: FBst0025781
UAS-ras85D.v12	Bloomington Drosophila Stock Center	BDSC: 4847
UAS-Sox100B	Fly ORF	FlyORF:F000238 Flybase: FBst0501530
UAS-Sox21a-RNAi	Bloomington Drosophila Stock Center	BDSC: 53991 Flybase: FBst0053991
UAS-Sox21a	Chen et al., 2016	N/A
NRE-Gal4^{ts},UAS-GFP	Zeng et al., 2010	N/A
esg-Gal4^{ts}	Goto and Hayashi, 1999	N/A
esg-Gal4^{ts}, UAS-GFP	Goto and Hayashi, 1999	N/A
Myo1A-Gal4^{ts},UAS-GFP	Jiang et al., 2009	N/A
ProsV1-Gal4, UAS-GFP	*from Bruce Edgar*	N/A
hs-flp;act < stop < Gal4,UAS-GFP;	Struhl and Basler, 1993	N/A
hsflp;Act-Gal4,UAS-EGFP;82B FRT-Gal80	Lee and Luo, 1999	N/A
UAS-upd	Harrison et al., 1995	N/A
UAS-hop	Harrison et al., 1995	N/A
UAS-Dome-DN	Brown et al., 2001	Flybase: FBal0126406
UAS-EGFR-DN	Freeman, 1996	N/A
UAS-EGFR-RNAi	Bloomington Drosophila Stock Center	BDSC:25781
UAS-EGFR$^{top4.2}$	Queenan et al., 1997	N/A
Sox21a-lacZ(GMR43E09)	Chen et al., 2016	N/A
UAS-EGFR	Fly ORF	FlyORF:F003563 Flybase: FBst0502619
UAS-Cic	Fly ORF	FlyORF:F001848 Flybase: FBst0501267
UAS-Cic-RNAi	Bloomington Drosophila Stock Center	BDSC:25995 Flybase: FBst0025995
UAS-Pdm1	Fly ORF	FlyORF:F000147 Flybase: FBst0501461
UAS-Pdm1-RNAi	Vienna Drosophila Resource Center	VDRC: 105044 Flybase: FBst0476872
UAS-Pdm1-RNAi	Vienna Drosophila Resource Center	VDRC: 101275 Flybase: FBst0473148
UAS-Pdm1-RNAi	Vienna Drosophila Resource Center	VDRC: 107814 Flybase: FBst0479627
NRE-lacZ	Zeng et al., 2010	N/A
Dl-Gal4	Zeng et al., 2010	N/A
UAS-P35	Bloomington Drosophila Stock Center	BDSC:5072
UASt-NLS-GFP-E2F1,UASt-NLS-RFP-CycB	Bloomington Drosophila Stock Center	BDSC:55121
UAS-Notch-RNAi	Bloomington Drosophila Stock Center	BDSC:7078
Sox100B^{del1}	This paper	N/A

(*Continued on next page*)

Continued

REAGENT or RESOURCE	SOURCE	IDENTIFIER
UAS-Sox100B(Chr. II)	This paper	N/A
UAS-Sox100B(Chr. III)	This paper	N/A
UAS-Dam	This paper	N/A
UAS-Dam-Sox100B	This paper	N/A
Sox100B-lacZ^{E1}	This paper	N/A
Sox100B-lacZ^{E2}	This paper	N/A
Sox100B-lacZ$^{E2\text{-}4n1}$	This paper	N/A
Sox100B-lacZ$^{E2\text{-}4n2}$	This paper	N/A
Sox100B-lacZ$^{E2\text{-}4n1,4n2}$	This paper	N/A
Sox100B-lacZ$^{E2\text{-}3n}$	This paper	N/A
Oligonucleotides		
Oligos used in this study are listed in Table S4	This paper	N/A
Recombinant DNA		
cDNA RT01136	Drosophila Genomics Resource Center	DGRC: 1623199 FlyBase: FBcl0383838
Plasmid: pCS2 oDam_f_GFPoNLS	Gutierrez-Triana et al., 2016	N/A
Plasmid: pUAST-Sox100B	This paper	N/A
Plasmid: UAS-Dam-attB-pUAST	This paper	N/A
Plasmid: UAS-Dam-Sox100B-attB-pUAST	This paper	N/A
Plasmid: C4PLZ-Sox100B-E1	This paper	N/A
Plasmid: C4PLZ-Sox100B-E2	This paper	N/A
Plasmid: C4PLZ-Sox100B-E2-4n1	This paper	N/A
Plasmid: C4PLZ-Sox100B-E2-4n2	This paper	N/A
Plasmid: C4PLZ-Sox100B-E2-3n	This paper	N/A
Plasmid: C4PLZ-Sox100B-E2-4n14n2	This paper	N/A
Software and Algorithms		
Prism	Graph Pad	https://www.graphpad.com/scientific-software/prism/
Adobe Photoshop CS5	Adobe	www.adobe.com/uk/products/photoshop.html
ImageJ	National Institutes of Health	https://imagej.net/Welcome
Adobe Illustrator CC 2014	Adobe	www.adobe.com/uk/products/Illustrator.html
Nikon Confocal Software	Nikon	https://www.microscope.healthcare.nikon.com/products/software/nis-elements/nis-elements-confocal
Leica Confocal Software	Leica	www.leica-microsystems.com/products/microscope-software/
R package iDEAR 2.0	Gutierrez-Triana et al., 2016	https://bitbucket.org/juanlmateo/idear
Other		
Raw and analyzed data: Cic-DamID-sequencing	Jin et al., 2015	GEO:GSE74188

RESOURCE AVAILABILITY

Lead Contact

Further information and requests for resources and reagents should be directed to and will be fulfilled by the Lead Contact, Rongwen Xi (xirongwen@nibs.ac.cn).

Materials Availability

All unique reagents generated in this study are available from the Lead Contact without restriction.

Data and Code Availability

The accession number for the mRNA and the iDam sequencing data reported in this paper is GEO: GSE130305. The accession number for the Cic-DamID sequencing data from a previous study is GEO: GSE74188 (Jin et al., 2015).

EXPERIMENTAL MODEL AND SUBJECT DETAILS

Drosophila melanogaster stocks were cultivated on standard media at room temperature and experimental crosses were performed at 25°C, unless otherwise specified. 5-10 days old female adult flies were collected for experiments and were transferred to fresh media with wet yeast paste added on the food surface every 2 days. Fly stocks and their resources are listed in the Key Resources Table. The following stocks were generated in this study: *Sox100B^{del1}, UAS-Sox100B, UAS-iDam, UAS-iDam-Sox100B, Sox100B-lacZ^{E1}, Sox100B-lacZ^{E2}, Sox100B-lacZ$^{E2\text{-}4n1}$, Sox100B-lacZ $^{E2\text{-}4n2}$, Sox100B-lacZ $^{E2\text{-}3n}$, Sox100B-lacZ $^{E2\text{-}4n1,4n2}$*.

METHOD DETAILS

Generation of Sox100B mutant flies and transgenic flies

Sox100B mutant flies were generated using CRISPR-cas9 system described previously (Kondo and Ueda, 2013). For Sox100B mutant generation, two guide RNAs were used to delete the fragment in between, and the Sox100^{del1} allele were generated with a 1037bp fragment (Chr. 3R 31,081,941-31,082,977) deletion, a frameshift mutation, in its coding region resulting in the removal of C-terminal 399 amino acids of the predicted 530 amino acid full length protein. The homozygous mutant flies are viable and fertile. For Sox100B-overexpressing transgenic fly generation, the amplified cDNA of Sox100B was then cloned into the pUAST vector with the transformation mediated by P-element or cloned into the attb-pUAST vector with the transformation mediated by phiC31. For UAS-iDam transgenic fly, the amplified cDNA of iDam was then cloned into the pUAST vector with the transformation mediated by P-element. For UAS-iDam-Sox100B transgenic fly generation, the cDNA of iDam was then cloned into the N-terminal of Sox100B in the pUAST-Sox100B vector with the transformation mediated by P-element. Fragments of every 2-3kb in length within or near the genomic region of *Sox100B* were cloned onto the C4PLZ vector with the transformation mediated by P-element for mapping enhancer regions of Sox100B. Purified plasmids were subsequently injected to relevant fly embryos. The oligonucleotides used in the study for generating those transgenic were listed in the Table S4.

Generation of Sox100B antibody

Polyclonal antibody against Sox100B was generated in rabbit using the following synthesized peptide: CEQQHQNPSQHHLWGTYTYVN. The cysteine residual was added into the N-terminal of the peptide and was used to conjugate keyhole limpet hemocyanin (KLH). Serum acquired from the immunized rabbit was purified by affinity chromatography and was used at a final dilution of 1:500.

Mosaic analysis

Gal4/UAS binary system and a temperature sensitive *Gal80* was used to temporally and spatially control transgene expression in specific cell types in fly midguts (Brand and Perrimon, 1993; McGuire et al., 2004). Flies were crossed and cultivated in 18°C and 5-10 days old adult female progenies with desired genotypes were shifted to 29°C for 7 days, unless otherwise specified, before dissection. MARCM system (Luo, 1999) and Flp/Out system (Struhl and Basler, 1993) were used to generate GFP-marked clones which were composed of mutant ISC and its progeny cells. Flies were crossed and cultivated in 25°C and 5-10 days old female progenies with desired genotypes were treated with 37°C heat-shock for 1 hour in water bath. Flies were shift back to 25°C for 7 days cultivation before dissection and analysis. For all mosaic experiments, we focused on the posterior midgut region for analysis.

Immunofluorescence staining

Immunofluorescence staining of fly midgut was performed as previously described (Lin et al., 2008). In brief, female flies were dissected in pre-cold PBS. The collected guts were fixed in 4% paraformaldehyde for 30 min and subsequently dehydrated in methanol at room temperature. Thereafter, primary antibodies were added in 5% NGS-PBT solution and incubated overnight at 4°C. Secondary antibodies were incubated at room temperature for 2 hours, followed by 5 min DAPI staining. Primary antibodies are listed in the Key Resources Table. Secondary antibodies include goat anti-rabbit, anti-mouse IgGs conjugated with Alexa Fluor 488, 568 or Cy5 (Invitrogen, Cat# A11034, A11036, A10524; 1:300) and donkey anti-goat IgGs conjugated with Alexa Fluor 555 (Invitrogen, Cat# A21432). Guts were washed in PBT (PBS with 0.1% Triton X-100) and were finally mounted by 75% glycerol. Images were captured by Nikon A1-R and Leica SP8 DLS confocal microscopes. Images were edited in Imag J, Adobe Photoshop and assembled in Adobe Illustrator.

DSS treatment

5-10 days old female flies were collected and then cultured with 5% sucrose solution with or without 5% DSS soaked Kimwipe paper at 29°C for 2 days, unless otherwise specified. Half of the flies were then dissected for analysis (damage phase), and another half were shift back to regular food and culture for another 1day or 4 days at 29°C before dissection and analysis (recovery phase) (Chen et al., 2016).

Enteric infection with Pe (Pseudomonas entomophila)

Enteric infection with *Pe* experiments were performed as previously described (Zielke et al., 2014). Briefly, a *Pe* colony was picked up to grow in 50ml Luria-Bartani (LB) medium overnight at 37°C and subsequently pelleted at 4000rpm for 10 min. The bacteria were resuspended using 5ml 5% sucrose-solution. 0.5 mL this *Pe* solution was then added to the fly food. As for control, 0.5 mL 5% sucrose solution was added to the fly food. 5-10 days old female flies were treated for 2 days. Half of the flies were then transfered to normal fly food for 1 or 4 days (recovery) before analysis.

Fluorescence intensity measurement

The ImageJ software was used to measure the fluorescence intensity of cells of interest as previously described (Chen et al., 2016). Briefly, the readout fluorescence intensity relative to background was calculated as the corrected fluorescence intensity divided by the corrected fluorescence intensity of the average background in the same cell nests. The corrected fluorescence intensity is the average fluorescence intensity of each cell's nuclear region minus the average of background fluorescence intensity.

Real time quantitative PCR (RT-qPCR) for gene expression analysis

5-10 days old female flies with desired genotypes were collected and shifted to the restriction temperature for 2-3 days before dissection, unless otherwise noted. Flies were dissected in ice-cold DEPC-PBS. Midguts were collected to homogenize in 400 μL RNAiso Plus (Takara, # 9109) buffer using glass pestle. 15-20 midguts were used for each sample, and 3 independent replicates were carried out for each experiment. Afterward, total RNA was extracted using Direct-zol RNA MiniPrepkit (Zymo Research, #R2050) according to the manufacturer's instructions, and on-column DNase I treatment was used to avoid genomic DNA contamination. For each sample, 1 μg RNA was used for *in vitro* transcription using 5X All-In-One RT Master Mix (abm, #G485) according to the manufacturer's instruction, and RT-qPCR was then carried out using SYBR Green PCR Master Mix (Applied Biosystems, #4309155) on an ABI PRISM 7500 Fast Real-Time PCR System (Applied Biosystems). Expression levels of genes were normalized to GAPDH. Primers used in this study were listed in the Table S4.

FACS and mRNA acquisition

Gene expression profiling of specific type of cells in *Drosophila* was performed follow a direction described before (Dutta et al., 2013). Briefly, female flies with genotype of esg^{ts}>*gfp*, esg^{ts}>*Sox100B-RNAi*, esg^{ts}>*Sox100B, ProsV1*>*GFP* and $Myo1A^{ts}$>*GFP* were collected and cultivated in 18°C for 5-10 days old and were then shifted to 29°C for 7 days (for esg>Sox100B-RNAi lines) or 3 days (for *esg*>*Sox100B*, *ProsV1*>*GFP* and $Myo1A^{ts}$>*GFP* lines). After that, fly midguts were dissected in the pre-cold DEPC-PBS within 2 hours and were digested with 1mg/ml elastase (Sigma, cat#E0258) for 1 hour at room temperature. Cells were pelleted at 300 g for 20min and resuspended in DEPC-PBS with 1mg/ml propidium iodide (PI) staining. Cell suspensions flowed through 40 μm filters (BD Falcon) and sorted using FACS Aria II sorter (BD Biosciences). W1118 midgut cells were used to set the fluorescent gate. PI^- GFP^+ live progenitor cells were collected into 300 μL RNA Extraction Buffer (Arcturus PicoPure RNA isolation kit). Arcturus PicoPure RNA isolation kit (Applied Biosystems) and Arcturus RiboAmp HS PLUS RNA amplification kit were used to harvest amplified mRNA. For each biological replicate, approximately 100 midguts were dissected and 20,000 cells were collected for RNA extraction and more than three replicates were performed for each genotype. RNA samples were subsequently sequenced by Illumina Hiseq-2500 system with 50 bp read length.

Bioinformatics analysis for RNA-seq data

Single-end reads were aligned against the *D. melanogaster* genome (Release 6) using STAR (v2.6.1a). Each sequencing experiment generated more than 20 million raw reads, and 92.5% was uniquely mapped for each experiment. Gene expression was quantified by the number of reads that fall into the exons and was normalized to RPKM (reads per kilobase of exon model per million mapped reads) using edgeR (v3.24.1). Significantly differentially expressed genes were identified with FDR $\leq$ 0.05 and fold change $\geq$ 2 by edgeR.

iDamID and bioinformatics analysis

iDamID analysis was carried out as previously described (Gutierrez-Triana et al., 2016; Li et al., 2020). Briefly, female flies with genotypes of esg^{ts}>*iDam*, and esg^{ts}>*iDam-Sox100B* were dissected to obtain midguts 2 days after transgene expression at adult stage. About 60 midguts were collected for gDNA isolation, followed by DpnII digestion and alkaline phosphatase treatment. Purified samples were additionally digested with DpnI and ligated with adaptor. Then, a ligation-mediated polymerase chain reaction (LM-PCR) was performed to amplify the gDNA samples and followed by T7 exonuclease treatment. The purified samples were treated with non-contact ultrasonic to break the gDNA fragments below 500bp.

Sequenced reads were mapped to the *D. melanogaster* genome (BDGP6) using bowtie2 (version 2.2.4). R package iDEAR 2.0 was used for establishing highly reliable profiles of transcription factor-binding sites. The density of reads in each region was normalized to the total number of 10 million mapped reads. BigWig files were generated for visualization using the Homer package.

QUANTIFICATION AND STATISTICAL ANALYSIS

All images displayed or collected for quantification are from the posterior midgut region (R4-5), unless otherwise specified. ImageJ was used to measure the fluorescence intensity of cells of interest. Graphpad Prism6 was used for statistical analysis and graphical representations based on three or more replicates for each experiment. All significance tests were carried out with unpaired two-tailed Student's t tests, mean ± SEM. Significance P values: $^{ns}p > 0.05$, $*p < 0.05$, $**p < 0.01$, $***p < 0.001$, $****p < 0.0001$.